data regarding the predominance of infection with HBV genotype D in Egypt [Saudy et al., 2003]. In addition, the phylogenetic analysis documented the presence of three different patterns of HBV genotype D transmission within the families in Egypt; maternal transmission (from mother to child as in the family 4), paternal transmission (from father to child as in family 35 and family 43) and spousal transmission (between spouses as in family 19 and family 37). This was different from the transmission pattern characteristics of genotype D in Uzbekistan where the horizontal transmission was the predominant route of infection with HBV genotype D within a family [Avazova et al., 2008].

The Data regarding the difference of transmission routes of HBV infection between different genotypes are controversial and scarce. Based on the findings that the patients infected with HBV genotype C may exhibit delayed HBeAg seroconversion decades later than the patients infected with other genotypes, Livingston et al. [2007] speculated that genotype C is the most responsible for the perinatal transmission and that the other genotypes (A, B, D, and F) are mainly transmitted horizontally [Livingston et al., 2007]. A recent study has shown a different data through exploring that both genotypes B and C can be transmitted by maternal and horizontal routes [Wen et al., 2011]. Whether different HBV genotypes have different transmission routes remains a question, which needs further global studies to clarify this interesting and important issue.

In an attempt to evaluate the influence of the universal vaccination on the intra-familial HBV infection, it was surprising to find a high prevalence rate of HBsAg among the vaccinated members with no significant difference when compared to the unvaccinated group. In an agreement with the present data, El Sherbini et al. [2006] reported the unchangeable prevalence of HBsAg among the vaccinated school children across a decade despite the significant decrease of the anti-HBc rate [El Sherbini et al., 2006]. The possible explanation for this vaccine failure is the acquiring of the HBV infection in the lag period between the birth and the time of receiving the first HBV vaccine dose at the age of 2 months. Supporting our explanation is the recent data coming from Taiwan where a different HBV infection prophylactic strategy is applied by administrating the first dose of the HBV vaccine at birth with the administration of the hepatitis B immunoglobulin to the infants born to the HBeAg positive mother within 24 hr after birth. The recent study has clearly demonstrated that the current HBV prophylactic strategy in Taiwan was capable of reducing the intra-familial HBV transmission and reducing the overall HBsAg positive rate among the infants [Mu et al., 2011]. In Japan, the extension of the active and passive immunization to the babies born to HBeAg negative mother had greatly reduced the HBsAg prevalence to 0.2% of blood donors younger than 19 years old [Noto et al., 2003; Matsuura et al., 2009]. The present study recommends the changing of the current HBV prophylactic policy in Egypt. It would be needed to provide the first dose of the HBV vaccine at birth together with screening for HBV infection markers prenatally and administration of the HBIG to the infants born from HBeAg-positive mothers. The documented role of the HBV spousal transmission in the present study by the phylogenetic analysis (Family 19 and Family 37), coincides with the recent data conducted in Egypt that the first sexual contact with an infected spouse was a significant risk factor for infection with HBV among females and may further emphasize the importance of the premarital screening for HBV in Egypt [Paez Jimenez et al., 2009]. Investigating the " a" determinant region of viral isolates retrieved from the vaccinated members infected with HBV provides no evidence of breakthrough infection by previously reported vaccine escape mutant virus [Carman et al., 1990].

In conclusion, the present study has clearly explored the role of the HBV intra-familial transmission and spread in north Eastern Egypt. Three patterns of HBV transmission were determined in the current cohort infected with HBV genotype D; maternal, paternal, and spousal. The present study recommends the change of the current prophylactic policy against the HBV infection in Egypt by including the first dose of HBV vaccine at birth, screening of pregnant women for HBsAg and the administration of HBIG to the infants born from HBeAg positive mothers within 24 hr after birth. Further studies are needed globally to determine the transmission patterns of different HBV genotypes and locally in different districts in Egypt to explore the impact of familial transmission in HBV infection in Egypt.

## REFERENCES

Abdel-Wahab M, el-Enein AA, Abou-Zeid M, el-Fiky A, Abdallah T, Fawzy M, Fouad A, Sultan A, Fathy O, el-Ebidy G, elghawalby N, Ezzat F. 2000. Hepatocellular carcinoma in Mansoura-Egypt: Experience of 385 patients at a single center. Hepatogastroenterology 47:663–668.

Alizadeh AH, Ranjbar M, Ansari S, Alavian SM, Shalmani HM, Hekmat L, Zali MR. 2005. Intra-familial prevalence of hepatitis B virologic markers in HBsAg positive family members in Nahavand, Iran World J Gastroenterol 11:4857–4860.

Arthur RR, el-Sharkawy MS, Cope SE, Botros BA, Oun S, Morrill JC, Shope RE, Hibbs RG, Darwish MA, Imam IZ. 1993. Recurrence of Rift Valley fever in Egypt. Lancet 342:1149–1150.

Avazova D, Kurbanov F, Tanaka Y, Sugiyama M, Radchenko I, Ruziev D, Musabaev E, Mizokami M. 2008. Hepatitis B virus transmission pattern and vaccination efficiency in Uzbekistan. J Med Virol 80:217–224.

Bracho MA, Gosalbes MJ, Gonzalez F, Moya A, Gonzalez-Candelas F. 2006. Molecular epidemiology and evolution in an outbreak of fulminant hepatitis B virus. J Clin Microbiol 44:1288–1294.

Carman WF, Zanetti AR, Karayiannis P, Waters J, Manzillo G, Tanzi E, Zuckerman AJ, Thomas HC. 1990. Vaccine-induced escape mutant of hepatitis B virus. Lancet 336:325–329.

Chen DS. 1993. From hepatitis to hepatoma: Lessons from type B viral hepatitis. Science 262:369–370.

Custer B, Sullivan SD, Hazlet TK, Iloeje U, Veenstra DL, Kowdley KV. 2004. Global epidemiology of hepatitis B virus. J Clin Gastroenterol 38:S158–S168.

Datta S, Banerjee A, Chandra PK, Chakravarty R. 2007. Selecting a genetic region for molecular analysis of hepatitis B virus transmission. J Clin Microbiol 45:687; author reply 688.

Dumpis U, Holmes EC, Mendy M, Hill A, Thursz M, Hall A, Whittle H, Karayiannis P. 2001. Transmission of hepatitis B virus infection in Gambian families revealed by phylogenetic analysis. J Hepatol 35:99–104.

el Gohary A, Hassan A, Nooman Z, Lavanchy D, Mayerat X, el Ayat A, Fawaz N, Gobran F, Ahmed M, Kawano F, Ragheb M, Elkady A, Tanaka Y, Murakami S, Attia FM, Hassan AA, Hassan MF, Shedid MM, Abdel Reheem HB, Khan A, Mizokami M. 1995. High prevalence of hepatitis C virus among urban and rural population groups in Egypt. Acta Trop 59:155–161.

El Sherbini A, Mohsen SA, Seleem Z, Ghany AA, Moneib A, Abaza AH. 2006. Hepatitis B virus among schoolchildren in an endemic area in Egypt over a decade: Impact of hepatitis B vaccine. Am J Infect Control 34:600–602.

el-Zayadi A, Selim O, Rafik M, el-Haddad S. 1992. Prevalence of hepatitis C virus among non-A, non-B-related chronic liver disease in Egypt. J Hepatol 14:416–417.

el-Zayadi AR, Badran HM, Barakat EM, Attia Mel D, Shawky S, Mohamed MK, Selim O, Saeid A. 2005. Hepatocellular carcinoma in Egypt: A single center study over a decade. World J Gastroenterol 11:5193–5198.

Kao JH, Chen DS. 2002. Global control of hepatitis B virus infection. Lancet Infect Dis 2:395–403.

Lavanchy D. 2004. Hepatitis B virus epidemiology, disease burden, treatment, and current and emerging prevention and control measures. J Viral Hepat 11:97–107.

Lee WM. 1997. Hepatitis B virus infection. N Engl J Med 337:1733–1745.

Lin CL, Kao JH, Chen BF, Chen PJ, Lai MY, Chen DS. 2005. Application of hepatitis B virus genotyping and phylogenetic analysis in intrafamilial transmission of hepatitis B virus. Clin Infect Dis 41:1576–1581.

Livingston SE, Simonetti JP, Bulkow LR, Homan CE, Snowball MM, Cagle HH, Negus SE, McMahon BJ. 2007. Clearance of hepatitis B e antigen in patients with chronic hepatitis B and genotypes A, B, C, D, and F. Gastroenterology 133:1452–1457.

Matsuura K, Tanaka Y, Hige S, Yamada G, Murawaki Y, Komatsu M, Kuramitsu T, Kawata S, Tanaka E, Izumi N, Okuse C, Kakumu S, Okanoue T, Hino K, Hiasa Y, Sata M, Maeshiro T, Sugauchi F, Nojiri S, Joh T, Miyakawa Y, Mizokami M. 2009. Distribution of hepatitis B virus genotypes among patients with chronic infection in Japan shifting toward an increase of genotype A. J Clin Microbiol 47:1476–1483.

Milas J, Ropac D, Mulic R, Milas V, Valek I, Zoric I, Kozul K. 2000. Hepatitis B in the family. Eur J Epidemiol 16:203–208.

Miyakawa Y, Mizokami M. 2003. Classifying hepatitis B virus genotypes. Intervirology 46:329–338.

Mu SC, Wang GM, Jow GM, Chen BF. 2011. Impact of universal vaccination on intrafamilial transmission of hepatitis B virus. J Med Virol 83:783–790.

Norder H, Courouce AM, Magnius LO. 1994. Complete genomes, phylogenetic relatedness, and structural proteins of six strains of the hepatitis B virus, four of which represent two new genotypes. Virology 198:489–503.

Noto H, Terao T, Ryou S, Hirose Y, Yoshida T, Ookubo H, Mito H, Yoshizawa H. 2003. Combined passive and active immunoprophylaxis for preventing perinatal transmission of the hepatitis B virus carrier state in Shizuoka, Japan during 1980–1994. J Gastroenterol Hepatol 18:943–949.

Okamoto H, Tsuda F, Sakugawa H, Sastrosoewignjo RI, Imai M, Miyakawa Y, Mayumi M. 1988. Typing hepatitis B virus by homology in nucleotide sequence: Comparison of surface antigen subtypes. J Gen Virol 69:2575–2583.

Ozasa A, Tanaka Y, Orito E, Sugiyama M, Kang JH, Hige S, Kuramitsu T, Suzuki K, Tanaka E, Okada S, Tokita H, Asahina Y, Inoue K, Kakumu S, Okanoue T, Murawaki Y, Hino K, Onji M, Yatsuhashi H, Sakugawa H, Miyakawa Y, Ueda R, Mizokami M. 2006. Influence of genotypes and precore mutations on fulminant or chronic outcome of acute hepatitis B virus infection. Hepatology 44:326–334.

Paez Jimenez A, El-Din NS, El-Hoseiny M, El-Daly M, Abdel-Hamid M, El Aidi S, Sultan Y, El-Sayed N, Mohamed MK, Fontanet A. 2009. Community transmission of hepatitis B virus in Egypt: Results from a case–control study in Greater Cairo. Int J Epidemiol 38:757–765.

Poland GA, Jacobson RM. 2004. Clinical practice: Prevention of hepatitis B with the hepatitis B vaccine. N Engl J Med 351:2832–2838.

Salkic NN, Zildzic M, Muminhodzic K, Pavlovic-Calic N, Zerem E, Ahmetagic S, Mott-Divkovic S, Alibegovic E. 2007. Intrafamilial transmission of hepatitis B in Tuzla region of Bosnia and Herzegovina. Eur J Gastroenterol Hepatol 19:113–118.

Saudy N, Sugauchi F, Tanaka Y, Suzuki S, Aal AA, Zaid MA, Agha S, Mizokami M. 2003. Genotypes and phylogenetic characterization of hepatitis B and delta viruses in Egypt. J Med Virol 70: 529–536.

Schaefer S. 2005. Hepatitis B virus: Significance of genotypes. J Viral Hepat 12:111–124.

Seeger C, Mason WS. 2000. Hepatitis B virus biology. Microbiol Mol Biol Rev 64:51–68.

Shin IT, Tanaka Y, Tateno Y, Mizokami M. 2008. Development and public release of a comprehensive hepatitis virus database. Hepatol Res 38:234–243.

Stuyver L, De Gendt S, Van Geyt C, Zoulim F, Fried M, Schinazi RF, Rossau R. 2000. A new genotype of hepatitis B virus: Complete genome and phylogenetic relatedness. J Gen Virol 81: 67–74.

Sugauchi F, Mizokami M, Orito E, Ohno T, Kato H, Suzuki S, Kimura Y, Ueda R, Butterworth LA, Cooksley WG. 2001. A novel variant genotype C of hepatitis B virus identified in isolates from Australian Aborigines: Complete genome sequence and phylogenetic relatedness. J Gen Virol 82:883–892.

Sugiyama M, Tanaka Y, Kato T, Orito E, Ito K, Acharya SK, Gish RG, Kramvis A, Shimada T, Izumi N, Kaito M, Miyakawa Y, Mizokami M. 2006. Influence of hepatitis B virus genotypes on the intra- and extracellular expression of viral DNA and antigens. Hepatology 44:915–924.

Tajiri H, Tanaka Y, Kagimoto S, Murakami J, Tokuhara D, Mizokami M. 2007. Molecular evidence of father-to-child transmission of hepatitis B virus. J Med Virol 79:922–926.

Thakur V, Guptan RC, Malhotra V, Basir SF, Sarin SK. 2002. Prevalence of hepatitis B infection within family contacts of chronic liver disease patients – Does HBeAg positivity really matter? J Assoc Physicians India 50:1386–1394.

Thakur V, Kazim SN, Guptan RC, Malhotra V, Sarin SK. 2003. Molecular epidemiology and transmission of hepatitis B virus in close family contacts of HBV-related chronic liver disease patients. J Med Virol 70:520–528.

Thompson JD, Higgins DG, Gibson TJ. 1994. CLUSTAL W: Improving the sensitivity of progressive multiple sequence alignment through sequence weighting, position-specific gap penalties and weight matrix choice. Nucleic Acids Res 22:4673–4680.

Ucmak H, Faruk Kokoglu O, Celik M, Ergun UG. 2007. Intra-familial spread of hepatitis B virus infection in eastern Turkey. Epidemiol Infect 135:1338–1343.

Wen WH, Chen HL, Ni YH, Hsu HY, Kao JH, Hu FC, Chang MH. 2011. Secular trend of the viral genotype distribution in children with chronic hepatitis B virus infection after universal infant immunization. Hepatology 53:429–436.

Wu W, Chen Y, Ruan B, Li LJ. 2005. Gene heterogeneity of hepatitis B virus isolates from patients with severe hepatitis B. Hepatobiliary Pancreat Dis Int 4:530–534.

Zakaria S, Fouad R, Shaker O, Zaki S, Hashem A, El-Kamary SS, Esmat G, Zakaria S. 2007. Changing patterns of acute viral hepatitis at a major urban referral center in Egypt. Clin Infect Dis 44:e30–e36.

Zampino R, Lobello S, Chiaramonte M, Venturi-Pasini C, Dumpis U, Thursz M, Karayiannis P. 2002. Intra-familial transmission of hepatitis B virus in Italy: Phylogenetic sequence analysis and amino-acid variation of the core gene. J Hepatol 36:248–253.

Zekri AR, Hafez MM, Mohamed NI, Hassan ZK, El-Sayed MH, Khaled MM, Mansour T. 2007. Hepatitis B virus (HBV) genotypes in Egyptian pediatric cancer patients with acute and chronic active HBV infection. Virol J 4:74.

Zervou EK, Gatselis NK, Xanthi E, Ziciadis K, Georgiadou SP, Dalekos GN. 2005. Intrafamilial spread of hepatitis B virus infection in Greece. Eur J Gastroenterol Hepatol 17:911–915.

Zuckerman AJ. 1997. Prevention of primary liver cancer by immunization. N Engl J Med 336:1906–1907.

SCIENTIFIC REPORTS

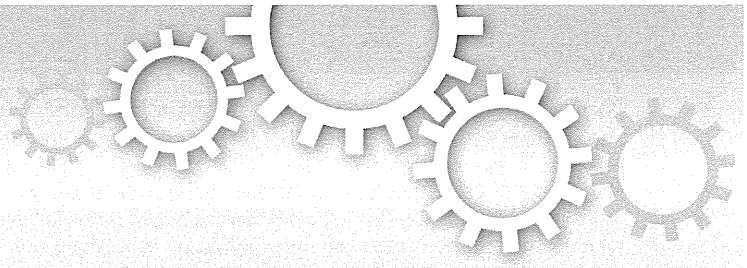

OPEN

SUBJECT AREAS:
GLYCOBIOLOGY
BIOCHEMICAL ASSAYS
ASSAY SYSTEMS
ELISA

Received
3 September 2012

Accepted
27 December 2012

Published
15 January 2013

Correspondence and requests for materials should be addressed to H.N. (h.narimatsu@aist.go.jp)

* These authors contributed equally to this study.

# A serum "sweet-doughnut" protein facilitates fibrosis evaluation and therapy assessment in patients with viral hepatitis

Atsushi Kuno[1]*, Yuzuru Ikehara[1]*, Yasuhito Tanaka[2], Kiyoaki Ito[3], Atsushi Matsuda[1], Satoru Sekiya[1], Shuhei Hige[4], Michiie Sakamoto[5], Masayoshi Kage[6], Masashi Mizokami[3] & Hisashi Narimatsu[1]

[1]Research Center for Medical Glycoscience (RCMG), National Institute of Advanced Industrial Science and Technology (AIST), Tsukuba, Japan, [2]Department of Virology & Liver Unit, Nagoya City University Graduate School of Medical Sciences, Nagoya, Japan, [3]The Research Center for Hepatitis and Immunology, National Center for Global Health and Medicine, Ichikawa, Japan, [4]Department of Internal Medicine, Hokkaido University Graduate School of Medicine, Sapporo, Japan, [5]Department of Pathology, School of Medicine, Keio University, Tokyo, Japan, [6]Department of Pathology, Kurume University School of Medicine, Kurume, Japan.

**Although liver fibrosis reflects disease severity in chronic hepatitis patients, there has been no simple and accurate system to evaluate the therapeutic effect based on fibrosis. We developed a glycan-based immunoassay, FastLec-Hepa, to fill this unmet need. FastLec-Hepa automatically detects unique fibrosis-related glyco-alteration in serum hyperglycosylated Mac-2 binding protein within 20 min. The serum FastLec-Hepa counts increased with advancing fibrosis and illustrated significant differences in medians between all fibrosis stages. FastLec-Hepa is sufficiently sensitive and quantitative to evaluate the effects of PEG-interferon-α/ribavirin therapy in a short post-therapeutic interval. The obtained fibrosis progression is equivalent to -0.30 stages/year in patients with sustained virological response, and 0.01 stages/year in relapse/nonresponders. Furthermore, long-term follow-up of the severely affected patients found hepatocellular carcinoma developed in patients after therapy whose FastLec-Hepa counts remained above a designated cutoff value. FastLec-Hepa is the only assay currently available for clinically beneficial therapy evaluation through quantitation of disease severity.**

The World Health Organization has estimated that the prevalence of chronic infections with hepatitis B virus (HBV) and hepatitis C virus (HCV) is more than 5% of the world population. The high rate of viral transmission worldwide has also resulted in an explosive increase in incidence of liver cirrhosis (LC), because liver fibrosis caused by the persistent infections with HBV and HCV irreversibly progresses in chronic hepatitis (CH) patients without effective treatment. As the incidence of hepatocellular carcinoma (HCC) increases proportionally to the severity of hepatitis and the presence of LC, it is now clear that about 90% of HCC cases originate from infection with HBV or HCV. It is estimated that more than one million patients worldwide die from liver disease related to HBV or HCV infection each year. Immunomodulatory therapy with PEG-interferon-α and ribavirin is the standard treatment for patients with chronic hepatitis C (CHC)[1]. Recent genome-wide association studies have revealed that variation in the host interleukin-28B gene can predict the outcome of therapies for viral clearance[2–4]. Such pharmacokinetic understanding should allow for more precise treatment protocols and follow-up analyses to optimize the opportunity for patients to achieve sustained virological response (SVR)[5,6]. Linear peptidomimetic HCV and NS3/4A serine protease inhibitors such as telaprevir and boceprevir are new drugs that, in combination with PEG-interferon-α and ribavirin, substantially improve the rates of response among patients with HCV genotype 1 infection[1]. Alternatively, suppression of hepatic decompensation in chronic hepatitis B patients with advanced fibrosis and cirrhosis has been evaluated during long-term treatment with antiviral agents, such as adefovir, lamivudine, entecavir, and tenofovir[7]. For example, cumulative entecavir therapy (for at least 3 years) resulted in substantial histological improvement and regression of fibrosis or cirrhosis[8].

The efficacy of therapy is currently evaluated by frequent monitoring of "viral load" or "liver injury"[5]. From the viewpoint of developing preventive strategies for HCC, the risk of HCC development should also be estimated along with them. For this purpose, liver biopsy is generally considered as the gold standard in which fibrosis is subclassified into 5 stages of severity (F0–4). However, this procedure is invasive and shown to cause a high rate of sampling error (about 15% false-negatives for cirrhosis) in patients with diffuse parenchymal liver diseases.

Furthermore, in a retrospective cohort study[9], the rate of fibrosis progression was estimated at about −0.28 stages/year in patients with SVR and 0.02 stages/year in patients with nonsustained virological response (NVR). This indicates that the biopsy is not suitable for evaluating the effect of therapy after a short interval. The procedure has further disadvantages such as inaccuracy, biopsy-related complications, the need for hospitalization, the time involved, and low cost-effectiveness[10]. Therefore, alternative noninvasive assays are desired and should provide a quantifiable readout of fibrosis progression using a method that is accurate, cost-effective and relatively simple.

To date, several methods have been developed[10] including FibroScan, which measures hepatic fibrosis biomechanically as tissue stiffness based on transient elastography. FibroScan has the advantages of being rapid and technically simple; however, its diagnostic success rate is affected by operator skill. Therefore, it has been suggested that FibroScan, in conjunction with assay of serum fibrosis biomarkers, should improve diagnostic accuracy. FibroTest[11] and FibroMeter[12], believed to be the most reliable indices of fibrosis, have been used in the combination assay aiming to eliminate the need for liver biopsy[13,14]. However, FibroTest and FibroMeter do not complement FibroScan in the development of a rapid "on-site diagnosis" system. This is because each requires both extensive and specialized blood analyses (FibroTest requires α2-macroglobulin, apolipoprotein A1, haptoglobin, γ-glutamyltransferase and total bilirubin whereas FibroMeter requires platelet count, prothrombin index, AST, α2-macroglobulin, hyaluronic acid and urea). In addition, both tests require data on age, and also sex for FibroTest.

Glycans are referred to as the face of cells, which reflect their status such as differentiation stage rather than their state of damage, and therefore they can be great markers for chronic disease. In the case of hepatitis, glycans are considered to reflect more specifically the progression of fibrosis than viral load. In the search for a simple and rapid method that is not markedly affected by tissue inflammation and ALT fluctuation, the possibility of glycomic and glycoproteomic techniques has emerged[15,16], and there are reports of some successful examples applicable for use in the clinical laboratories[17–19]. However, the current glycomic techniques require at least 3 hours of sample preparation for analysis and this has markedly reduced the combination use of glycan-based immunoassays with FibroScan. In this report, we describe for the first time, a rapid and simple glycan-based immunoassay, FastLec-Hepa, that can quantify fibrosis as precisely as FibroTest and also readily evaluate the antifibrotic effects of therapy at the clinical site (**Supplementary Fig. 1**). Moreover, we introduce a novel method for rational selection of the "non-fucose binding type" lectins and provide details of how this concept can be adopted for future development of clinically useful glycodiagnostic tools.

## Results

**Changes in the *N*-glycosylation of M2BP during progression of liver disease.** Based on previous reports[20–23], we adopted the serum 90 K/Mac-2 binding protein (M2BP) as a glycoprotein biomarker for liver fibrosis. M2BP is secreted from many cell types, including hepatocytes (http://www.proteinatlas.org/ENSG00000108679), and it has been shown to modulate many processes, particularly those related to cell adhesion. For example, the interaction of M2BP with matrix fibronectin can modulate adhesion and the high expression of M2BP by tumor cells increases the level in the circulation of affected patients. A prominent feature of native human M2BP is its oligomerization to large ring structures[20], resembling a "sugar-powdered doughnut" which is potentially covered with 70–112 *N*-glycans (**Fig. 1a**). To confirm serum M2BP as a valid marker, we performed a pull-down assay with serum (2 μl each) from five individuals in each of the following groups: HCC, LC, CHC or healthy volunteer with normal liver (HV). Although two bands appeared in all HVs and two CHC patients, M2BPs from patients with relatively severe fibrosis, i.e., LC and HCC, migrated as a single band, the mobility of which was similar to that of the lower band for HVs (**Fig. 1b**). Significant increases in band intensity with excessive smearing of the bands were seen for most HCC patients. A subsequent investigation of 125 HCV patients with stage-determined fibrosis showed alteration in the quality and quantity of M2BP during the progression of fibrosis (**Fig. 1c**) and apparent alteration in the amount of each band (**Fig. 1d and e**), as described in the previous investigations[22,23]. M2BP has been shown to have multibranching and sialylated *N*-glycans. Moreover, it has been suggested that extension of polylactosamine on M2BP controls its binding to galectin-3, a major binding partner *in vivo*. Sialylation and extension of polylactosamine affect the charge and size of M2BP and this results in altered electrophoretic migration. Accordingly, we speculate that the size heterogeneity of M2BP seen on electrophoresis is due to such alterations in glycosylation. In fact, the difference in the band migration was eliminated by Sialidase A treatment, and the smearing of the bands in HCC was reduced by treatment with *N*-Glycosidase F (**Supplementary Fig. 2**). These results indicated that the altered quality of M2BP during progression of liver disease was due to changes in *N*-glycosylation.

**Selection of the optimal lectin for direct measurement of disease-related M2BP.** To construct a reliable assay (see **Supplementary Fig. 3**), we needed to identify a lectin probe that could most readily discriminate the altered *N*-glycans of M2BP and specifically binds to them in serum without pretreatment. For this purpose, we added a subtraction process to our recently described microarray-based selection strategy[16] (**Supplementary Fig. 4**). In brief, we first obtained a typical glycan profile for serum M2BPs by averaging the glycan profiles of M2BPs immunoprecipitated from 125 HCV patient sera by the antibody-overlay lectin microarray[16,18,24] (**step 1**). In this step, we selected 27 lectins binding to M2BP from a 45-lectin array (**Supplementary Fig. 5a**). Most of them bound not only to M2BP (ca. 10 μg/ml in serum), but also to other abundant serum glycoproteins, whereas some suggested rather specific binding to M2BP. We designated them as high-noise lectins or high signal-to-noise (S/N) lectins, respectively (**Fig. 2a**). We then selected the candidate lectins for the assay by subtracting the high-noise lectins from the M2BP-binding lectins (**step 2**), using a glycan profile of whole serum (**Supplementary Fig. 5**)[25]. Comparing the profiles for M2BP and whole serum (**Fig. 2b**), we quickly identified 6 lectins with a high S/N ratio. Interestingly, all lectins identifying fucose modification, which is the most well-known glyco-alteration in liver disease (*Pisum sativum* agglutinin (PSA), *Lens culinaris* agglutinin (LCA), *Aspergillus oryzae* lectin (AOL), and *Aleuria aurantia* lectin (AAL)), were high-noise lectins (**Fig. 2b**). After subtraction, we used both the Mann–Whitney *U* test as a nonparametric test, and receiver-operating characteristic (ROC) analysis, to characterize the diagnostic accuracy of the candidate lectins at each stage of fibrosis: significant fibrosis (F2/F3/F4), severe fibrosis (F3/F4) and cirrhosis (F4) (**step 3**). As a result, we found that the diagnostic score of *Wisteria floribunda* agglutinin (WFA) was superior to the other 5 lectins at every fibrosis stage (**Fig. 2c and Supplementary Fig. 6**).

**"Proof-of-concept" experiment for direct quantitation of the serum WFA-binding M2BP by sandwich immunoassay.** We quantitatively analyzed the WFA-binding M2BPs ($WFA^+$-M2BP) in serum. Sera, pretreated as described in the **Methods**, were firstly subjected to affinity capture with 20 μl slurry of WFA-coated agarose gel. The eluted fraction was immunoprecipitated with a capturing antibody against M2BP and the product was analyzed by Western blot. The intensity of the "smearing-band" signal for $WFA^+$-M2BP gradually increased in proportion to the severity of liver fibrosis (**Supplementary Fig. 7**), as indicated by the red line shown in

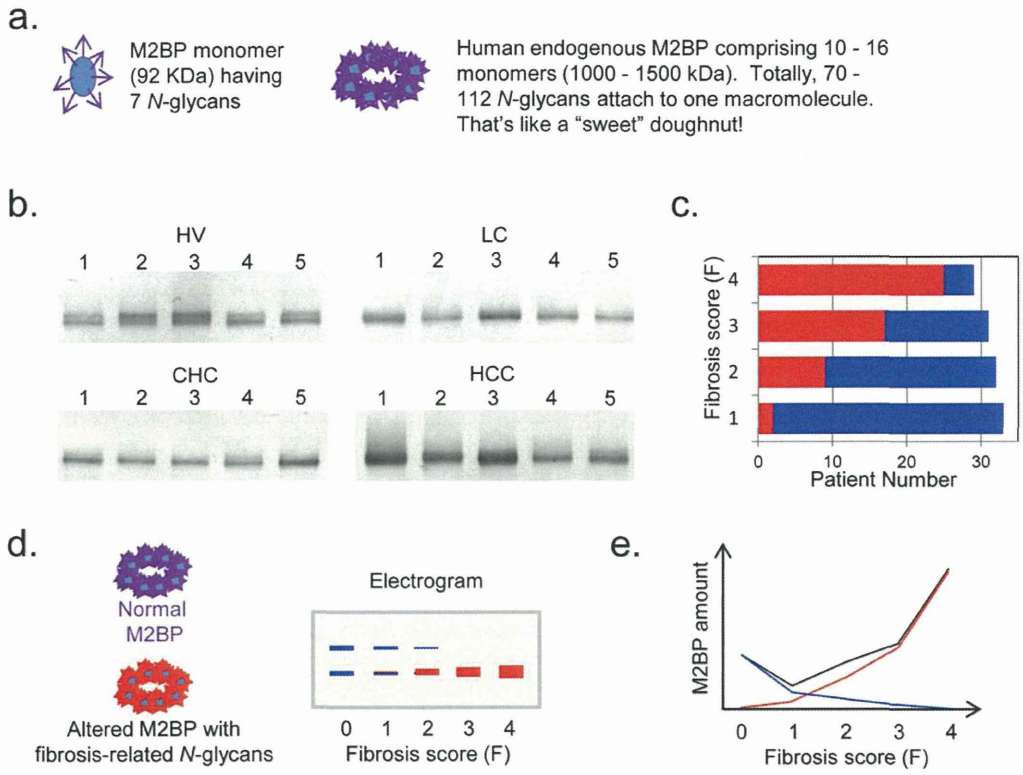


**Figure 1 | Changes in the quality and quantity of human serum M2BP with progression of liver fibrosis.** (a) The unique shape of human endogenous serum M2BP. The arrowheads and circles represent the *N*-glycan moieties and core protein respectively. (b) Western blot analysis: M2BPs in 2 μl of serum were purified by immunoprecipitation before SDS-PAGE. HV, healthy volunteer; CHC, patient with chronic hepatitis C; LC, HCV-infected patient with liver cirrhosis; and HCC, HCV-infected patient with hepatocellular carcinoma. (c) Number of patients with single (red) or double (blue) band appearance on the blot. The number of bands was determined visually by two independent analysts. The total number of HCV patients who participated in this study was 125 (F0–F1 [$n = 33$], F2 [$n = 32$], F3 [$n = 31$], and F4 [$n = 29$]). (d) Typical changes of serum M2BP band intensities in patients with different fibrosis scores and (e) concentrations based on a previous report on quantitation of serum M2BP by Cheung *et al*[3]. and our present results. The blue bands on the electrogram and blue line on the graph represent M2BPs secreted from normal liver. The red bands and line represent altered M2BP, the concentration of which is suggested to increase with the progression of fibrosis. The black line represents the total concentration of serum M2BP.

**Fig. 1e**. We next conducted a sandwich immunoassay with WFA and anti-M2BP antibody (see **Supplementary Fig. 3b**). WFA was immobilized on the surface of a 96-well microtiter plate through biotin–streptavidin interaction. We performed the first assay for the WFA-binding activity using recombinant human M2BP (rhM2BP). As a result, a linear regression analysis revealed a linear range of detection from 0.039 to 0.625 μg/ml (**Supplementary Fig. 8a**). Subsequently, we used culture supernatant of a hepatoblastoma cell line HepG2, which expresses $WFA^+$-M2BP, to illustrate the dose-dependency of the interaction of WFA with M2BP/HepG2. We also showed that heat treatment of the culture supernatant eliminated this binding activity (**Supplementary Fig. 8b**). Finally, we performed a sandwich immunoassay for direct measurement of $WFA^+$-M2BP in untreated serum samples, and the results correlated well with the quantitative assay using affinity capture and lectin microarray analysis (**Supplementary Fig. 7 and 9**).

**FastLec-Hepa: a fully automated sandwich immunoassay for direct quantitation of serum $WFA^+$-M2BP.** We adapted the WFA-antibody immunoassay to the HISCL-2000i bedside clinical chemistry analyzer[18]. We successfully adjusted every reaction condition during the automatic assay by HISCL, which is about a 17-min manipulation. Heat pretreatment of the serum was avoided to ensure both binding avidity and the fast association rate. Repeatability was assessed by performing 10 independent assays of three samples, and the coefficient of variation ranged between 2.1% and 2.5% (data not shown). Sensitivity was determined by triplicate assays of samples generated by 2-fold serial dilution of 50 μg/ml rhM2BP. The linear regression analysis identified a linear range of detection ($R^2 = 1.00$) from 0.025 to 12.5 μg/ml (**Fig. 3a**, a range of 0.025 to 1.6 μg/ml also shown in **Fig. 3b**). The resulting dynamic range was 25-fold that of the manual sandwich immunoassay described above. We next examined whether the HISCL measurements made on serum from HCV patients ($n = 125$) were consistent with lectin microarray analysis, and this comparison resulted in sufficient linearity with coefficient of determination, $R^2 = 0.848$ (**Fig. 3c**). Accordingly, we could perform automatic quantitation of serum $WFA^+$-M2BP in 180 patients in 1 hour and we have therefore named it FastLec-Hepa.

**Validation of FastLec-Hepa.** For a validation study, we obtained serum from CH patients at two locations: Nagoya City University Hospital and Hokkaido University Hospital (**Supplementary Fig. 10**). Staging of these patients ($n = 209$) by histological activity index (HAI) was conducted independently by two senior pathologists on ultrasonography-guided liver biopsy samples. F0–F1 was assigned in 82 cases (39.2%), F2 in 52 (24.9%), F3 in 40 (19.1%), and F4 (cirrhosis) in 35 (16.7%). Serum from healthy volunteers (with no history of any hepatitis virus infections) was obtained for analysis from two sites ($n = 48$ from National Institute of Advanced Industrial Science and Technology [AIST]: HV1; $n = 70$ from Nagoya City University: HV2). Their FastLec-Hepa counts

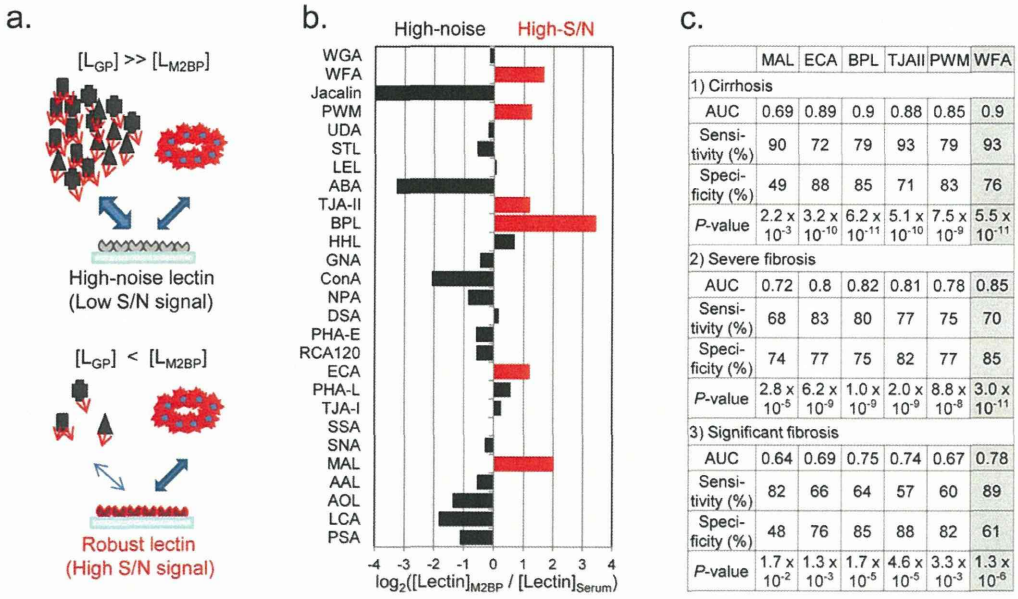


c.

| | MAL | ECA | BPL | TJAII | PWM | WFA |
|---|---|---|---|---|---|---|
| 1) Cirrhosis | | | | | | |
| AUC | 0.69 | 0.89 | 0.9 | 0.88 | 0.85 | 0.9 |
| Sensitivity (%) | 90 | 72 | 79 | 93 | 79 | 93 |
| Specificity (%) | 49 | 88 | 85 | 71 | 83 | 76 |
| *P*-value | $2.2 \times 10^{-3}$ | $3.2 \times 10^{-10}$ | $6.2 \times 10^{-11}$ | $5.1 \times 10^{-10}$ | $7.5 \times 10^{-9}$ | $5.5 \times 10^{-11}$ |
| 2) Severe fibrosis | | | | | | |
| AUC | 0.72 | 0.8 | 0.82 | 0.81 | 0.78 | 0.85 |
| Sensitivity (%) | 68 | 83 | 80 | 77 | 75 | 70 |
| Specificity (%) | 74 | 77 | 75 | 82 | 77 | 85 |
| *P*-value | $2.8 \times 10^{-5}$ | $6.2 \times 10^{-9}$ | $1.0 \times 10^{-9}$ | $2.0 \times 10^{-9}$ | $8.8 \times 10^{-8}$ | $3.0 \times 10^{-11}$ |
| 3) Significant fibrosis | | | | | | |
| AUC | 0.64 | 0.69 | 0.75 | 0.74 | 0.67 | 0.78 |
| Sensitivity (%) | 82 | 66 | 64 | 57 | 60 | 89 |
| Specificity (%) | 48 | 76 | 85 | 88 | 82 | 61 |
| *P*-value | $1.7 \times 10^{-2}$ | $1.3 \times 10^{-3}$ | $1.7 \times 10^{-5}$ | $4.6 \times 10^{-5}$ | $3.3 \times 10^{-3}$ | $1.3 \times 10^{-6}$ |

**Figure 2 | Selection of the optimal lectin for the lectin-antibody sandwich immunoassay.** (a) The kinetics of lectins binding to serum glycoproteins. The M2BP-binding lectins are divided into two categories: high-noise lectins and high signal-to-noise (S/N) lectins. The high-noise lectins bind to both M2BPs and abundant serum glycoproteins, causing a strong suppression of the M2BP–lectin interaction (see *top panel*). On the other hand, the number of binding targets in serum for the high S/N lectins is negligible, resulting in the specific interaction with the target M2BP (see *lower panel*). (b) Classification of M2BP-binding lectins. The high S/N lectins are those detecting M2BPs with at least twice the signal intensity seen for other serum glycoproteins. The classification strategy is summarized in **Supplementary Fig. 4**. (c) Diagnostic performance of 6 candidate lectins. *P*-values were determined using the nonparametric Mann–Whitney *U* test (Excel 2007, Microsoft).

(**Supplementary Table 1**) are also plotted in a box-whisker diagram in **Supplementary Fig. 11** along with that from a separate group of 1,000 healthy volunteers (HV3). Based on the calibration curve ([FastLec-Hepa counts]/$10^6$ = 1.027 × [rhM2BP] + 0.006 in **Fig. 3a, b**), the 75$^{th}$ percentiles of HVs of 64,205–107,617 and the 25$^{th}$ percentile of LC of 1,327,596 patients (see also **Supplementary Fig. 11**), we estimate the concentration of WFA$^+$-M2BP to be approximately 0.09 μg/ml in the serum of HV patients and > 1.0 μg/ml in that of LC patients. This means that the linear range shown in **Fig. 3a** is sufficient for accurate quantitation of WFA$^+$-M2BP in all serum samples. The analyses showed a gradual increase with the progression of liver fibrosis, but it did not correlate with the grade of hepatic activity defined by HAI scoring (**Supplementary Fig. 12**).

Next, we made a statistical comparison of FastLec-Hepa with other simple tests for liver fibrosis: the direct fibrosis marker hyaluronic acid (HA), the indirect fibrosis index FIB-4[26] and the glycan-based fibrosis index LecT-Hepa[18,27]. We enrolled 160 patients (F0−F1 = 66, F2 = 41, F3 = 33 and F4 = 20) whose age, platelet count, AST, ALT and HA levels were readily available (**Supplementary Fig. 10** and **Supplementary Tables 1 and 2**). As shown in **Fig. 4a**, the results of all the tests correlated well with the stage of fibrosis ($P < 0.0001$). However, an ROC analysis concluded that FastLec-Hepa detected cirrhosis with the highest diagnostic accuracy (**Fig. 4b** and **Table 1**). Notably, FastLec-Hepa distinguished between F3 and F4 with 90% sensitivity, 85% specificity, and with an AUC of 0.91. These results were superior to LecT-Hepa (sensitivity:

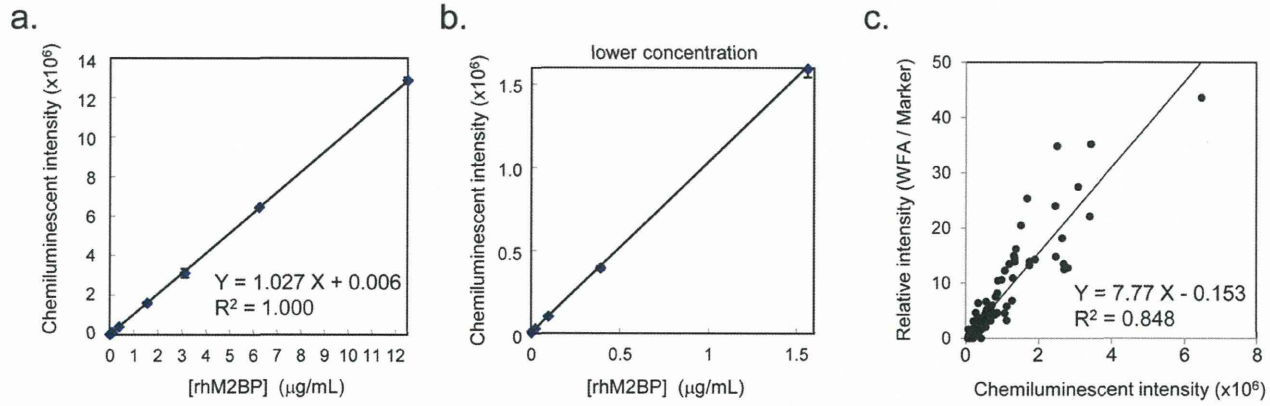


**Figure 3 | Description of FastLec-Hepa, a fully automated WFA and anti-M2BP antibody sandwich immunoassay.** (a) Standard curve for quantitation of WFA-binding rhM2BP. Plots for the lower concentration of rhM2BP are alternatively highlighted in (b). (c) Scatterplot comparison of WFA$^+$-M2BP data obtained from 125 different serum samples by both HISCL and a manual lectin microarray assay. The best-fit linear comparison with its correlation coefficient was calculated in Excel 2007 (Microsoft).

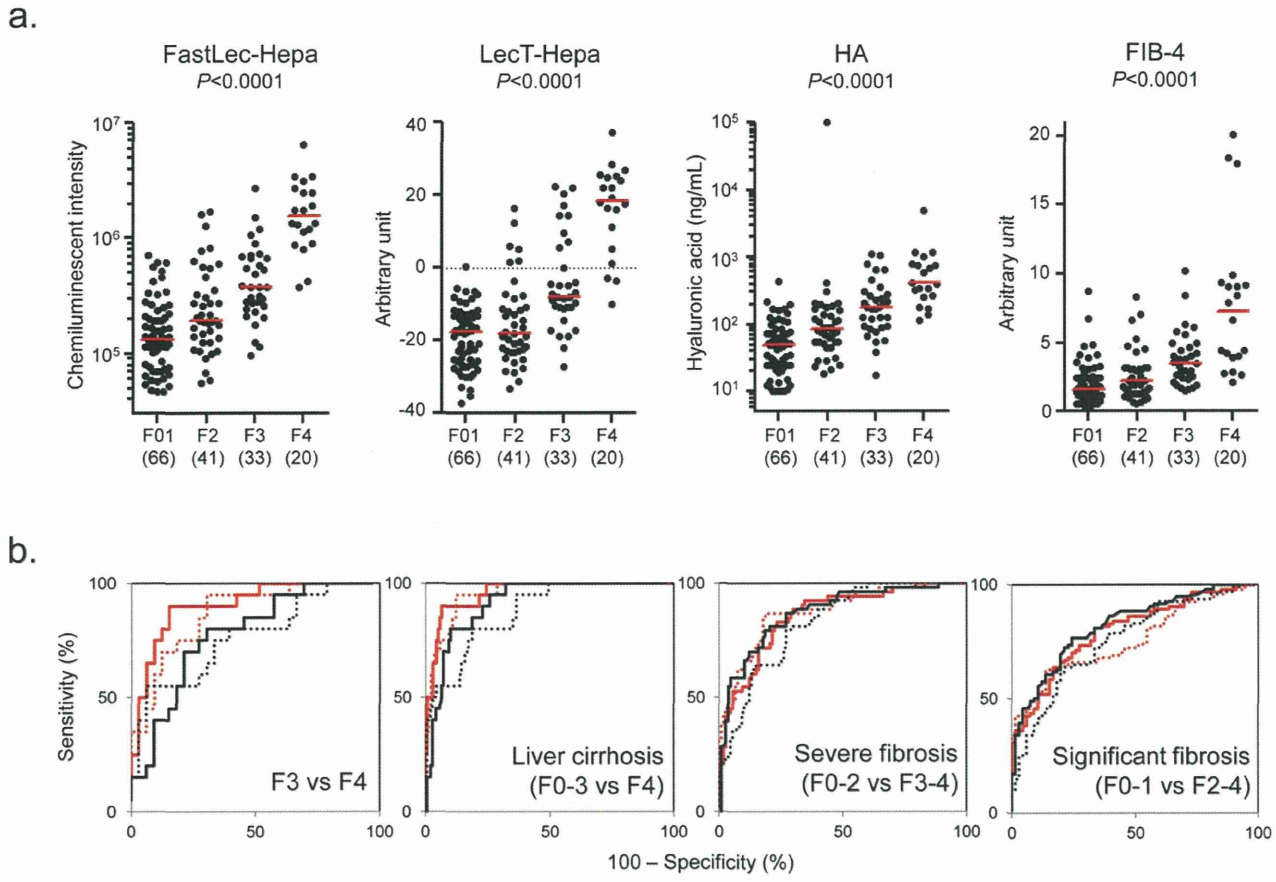


**Figure 4 | Comparison of diagnostic performance of FastLec-Hepa, LecT-Hepa, HA, and FIB-4.** (a) Scatterplots of the data obtained with FastLec-Hepa, LecT-Hepa, HA, and FIB-4 against the fibrosis score. Red horizontal lines represent the median. Correlation of the data with the progression of fibrosis was evaluated as significant differences in the medians relative to the fibrosis scores ($P < 0.0001$) by a nonparametric method, the Kruskal–Wallis one-way ANOVA. (b) Area under the receiver-operating characteristic (AUC-ROCs) curves of FastLec-Hepa, LecT-Hepa, HA, and FIB-4 for liver cirrhosis (F3 vs F4 or F0–3 vs F4), severe fibrosis (F0–2 vs F3–4), and significant fibrosis (F0–1 vs F2–4). FastLec-Hepa, LecT-Hepa, HA, and FIB-4 are indicated by a red solid line, red dotted line, black solid line, and black dotted line, respectively.

95%, specificity: 70%, and AUC: 0.87), FIB-4 (sensitivity: 55%, specificity: 94%, and AUC: 0.76), and HA (sensitivity: 80%, specificity: 70%, and AUC: 0.78).

**Clinical utility of FastLec-Hepa: quantitative monitoring of antiviral therapy.** To assess clinical utility, we examined two types of trials—short-interval evaluation and long-term follow-up—both of which are essential for following the patients receiving PEG-interferon-α and ribavirin therapy. For the first trial, we enrolled 41 patients with CHC who had previously undergone 48 weeks of therapy at Hokkaido University Hospital. According to the definition described in the **Methods**, 26 and 15 of them were judged as SVR and NVR/relapse (non-SVR), respectively. For each patient, we performed FastLec-Hepa on serum samples, which were collected just before treatment (Pre) and within a short period (12–22 weeks) after treatment (Post) (**Fig. 5a**). We found a marked decrease from Pre to Post counts ($P = 0.0061$) in SVR patients, but no apparent change for non-SVR patients ($P = 0.9780$) (**Fig. 5b**). Specifically, a median percent decrease of 31% was found for SVR patients (median Pre-count of 161,053 and median Post-count of 110,739), while the level for non-SVR patients was essentially constant. These results show that the assay can evaluate the effect of therapy within a short period after treatment. This is an important advance, because the ALT levels of non-SVR, as well as SVR, are mostly decreased into the range of 10–64 IU/ml during this period (**Fig. 5c**)[5]. In fact, changes in the FastLec-Hepa counts did not correlate with those in the ALT counts (**Supplementary Fig. 13**), thereby invalidating ALT-dependent fibrosis assays, including FIB-4 (**Fig. 5d**).

In support of our finding that the FastLec-Hepa counts correlate excellently with the stage of fibrosis, we found a strong correlation between the histopathological scores and the median of the $\log_{10}$[FastLec-Hepa] counts (**Fig. 5e**). These correlations were approximated to two linear equations: $y = 0.23x + 4.9$ for F0 to F3, and $y = 0.58x + 3.8$ for F3 to F4 histology. This means that FastLec-Hepa can reliably reproduce the assessment of therapeutic effects, which were previously drawn from histopathological scoring[9]. Indeed, the median changes in fibrosis obtained by FastLec-Hepa analysis were about −0.295 stages/year for SVR and 0.010 stages/year for non-SVR (**Fig. 5f**). These data were consistent with the rate of fibrosis progression and regression determined by Shiratori *et al*[9].

For the second trial, we enrolled 6 HCV patients (SVR = 3 and non-SVR = 3) with advanced fibrosis who completed 48 weeks of therapy at Nagoya City University Hospital. Sera were collected before therapy and at 0, 1, 3, and 5 years after the end of therapy (see **Fig. 5g**). FastLec-Hepa counts in SVR patients gradually decreased and reached below the median of F0 patients within 3 years. However, those in non-SVR patients remained above the median for F3 patients during the follow-up period (**Fig. 5h**).

Table 1 | Diagnostic performance of fibrosis markers

| $n = 160$ | FIB-4 | HA | LecT-Hepa | FastLec-Hepa |
|---|---|---|---|---|
| a) Significant fibrosis (F0–1 vs F2–4) | | | | |
| AUC | 0.76 | 0.82 | 0.76 | 0.79 |
| (95% CI) | (0.68–0.83) | (0.76–0.89) | (0.69–0.83) | (0.72–0.86) |
| Diagnostic sensitivity (%) | 64 | 77 | 63 | 81 |
| Diagnostic specificity (%) | 79 | 76 | 86 | 67 |
| Youden's index (%) | 43 | 52 | 49 | 48 |
| b) Severe fibrosis (F0–2 vs F3–4) | | | | |
| AUC | 0.83 | 0.87 | 0.88 | 0.84 |
| (95% CI) | (0.76–0.89) | (0.81–0.93) | (0.82–0.93) | (0.77–0.91) |
| Diagnostic sensitivity (%) | 81 | 81 | 87 | 83 |
| Diagnostic specificity (%) | 71 | 79 | 81 | 77 |
| Youden's index (%) | 52 | 61 | 68 | 60 |
| c) Liver cirrhosis (F0–3 vs F4) | | | | |
| AUC | 0.88 | 0.91 | 0.95 | 0.96 |
| (95% CI) | (0.80–0.95) | (0.86–0.96) | (0.92–0.99) | (0.93–0.99) |
| Diagnostic sensitivity (%) | 80 | 80 | 95 | 90 |
| Diagnostic specificity (%) | 81 | 90 | 88 | 94 |
| Youden's index (%) | 61 | 70 | 83 | 84 |
| d) Liver cirrhosis (F3 vs F4) | | | | |
| AUC | 0.76 | 0.78 | 0.87 | 0.91 |
| (95% CI) | (0.63–0.90) | (0.65–0.90) | (0.77–0.97) | (0.82–0.99) |
| Diagnostic sensitivity (%) | 55 | 80 | 95 | 90 |
| Diagnostic specificity (%) | 94 | 70 | 70 | 85 |
| Youden's index (%) | 49 | 50 | 65 | 75 |

Interestingly, HCC had developed in two non-SVR patients whose FastLec-Hepa counts remained above the median of F4 patients throughout. Other fibrosis indices, such as FIB-4 and biochemical parameters (ALT and AST), did not distinguish between SVR and non-SVR or appear to predict this occurrence (**Fig. 5i-k**).

## Discussion

We have described the development and use of a fully automated, glycan-based immunoassay termed FastLec-Hepa, for the evaluation of liver fibrosis. A high degree of reliability in the quantitative aspects of this method should establish it as a clinically significant test,

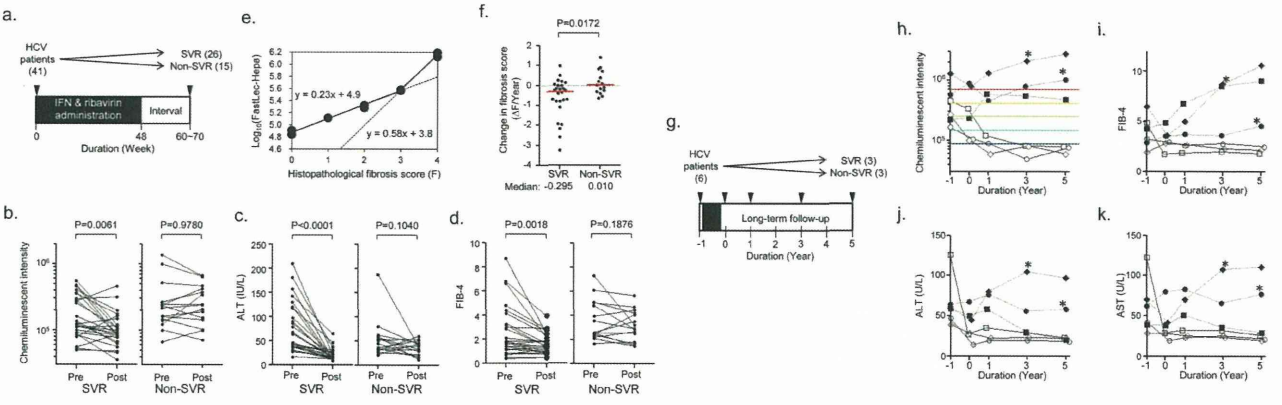


**Figure 5 | Evaluation of the curative effect of interferon therapy by FastLec-Hepa.** (a) Validation of FastLec-Hepa in short-interval evaluation. The numbers in parentheses represent the number of patients participated in this experiment. Arrowheads indicate the timing of blood collection. At week 0, blood was collected immediately before the treatment. Black box indicates the period of PEG-interferon-α and ribavirin therapy. Changes in the FastLec-Hepa counts (b), ALT (c), and the FIB-4 index (d) in patients with sustained virologic response (SVR) and relapse/nonresponders (non-SVR) during interferon therapy. The *P*-value was determined by a nonparametric method, the Wilcoxon matched pairs signed-rank test. (e) Dot-plot representation of the histopathological fibrosis score and the medians of FastLec-Hepa counts. Best-fit linear curves were calculated in Excel 2007 (Microsoft) allowing conversion of the FastLec-Hepa counts into fibrosis score. (f) Yearly changes in the converted fibrosis score. Changes for patients with SVR and non-SVR are indicated in the dot plots. Red horizontal lines represent the median. The *P*-value was determined by the Mann–Whitney *U* test. (g) Validation of FastLec-Hepa in long-term follow-up. The numbers in parentheses represent the number of patients participated in this experiment. Arrowheads indicate the timing of blood collection. At year -1 and 0, the blood was collected immediately before and after the treatment, respectively. Black box indicates the period of PEG-interferon-α and ribavirin therapy. Yearly changes of FastLec-Hepa counts (h), FIB-4 index (i), ALT (j), and AST (k) in individual patients after therapy. The five colored lines in (h) represent the median values obtained for each fibrosis stage (red, F4; orange, F3; green, F2; cyan, F1; blue, F0). Closed and opened symbols indicate the data obtained from non-SVR and SVR patients, respectively. * indicates the period when the development of HCC was found.

particularly for revealing and managing patients at a high risk of progression to liver complications such as HCC and related life-threatening events. The most striking advantage of FastLec-Hepa is not only its simplicity but also its capacity to provide fibrosis read-outs that are not influenced by fluctuations in the ALT value or inflammation, both of which can cause falsely high estimates in most of the other fibrosis tests available[10]. In fact, our study has illustrated robust capacity of FastLec-Hepa to evaluate the effects of antiviral therapy and subsequent disease progression in both the short and long term.

Many retrospective and prospective studies have demonstrated that achieving SVR through the PEG-interferon-α/ribavirin treatment significantly reduces liver-related morbidity and mortality (i.e., hepatic decompensation, HCC, and liver-related death)[28–30]. As this combination therapy is effective in only about 50% of patients with HCV genotype 1, new agents[1] and targets[31] for antiviral treatments of HCV have been developed to achieve SVR more effectively after the therapy. Long-term follow-ups often show that the risk of disease progression is significantly high in patients with non-SVR after PEG-interferon-α/ribavirin treatment. Furthermore, the development of HCC in patients with SVR remains at a significant cumulative rate (2%)[28,30,32,33]. For these reasons, a new data-mining model using individual factors (age, platelet count, serum albumin and AST) was developed recently to identify patients at a high risk of HCC development[34]. This is, however, a statistical procedure for estimating the chance of disease progression, and there is not a direct evaluation of fibrosis. In the present report, we performed a long-term retrospective study with serially collected sera from SVR and non-SVR patients, in which we showed the potential use of FastLec-Hepa for improved prognostic accuracy. Indeed, recent advances in the development of antifibrotic agents lead us to expect the therapeutic elimination of health risks associated with HCC and decompensation[35]. Moreover, we expect that FastLec-Hepa will be proved for its usefulness in rapid evaluation of progression and regression of fibrosis in clinical trials of newly developed antifibrotic agents. Hence, FastLec-Hepa should be very useful for fibrosis stage screening and evaluation of disease progression in untreated individuals or patients under or after treatment, as well as evaluation of the most recently developed drugs.

It is important to note that FastLec-Hepa has many merits, including speed (possibly 1,000 assays per day) and full automation for measurement of a serological glycobiomarker: these attributes will enable retrospective studies with valuable serum specimens that have been collected previously. In addition, our recently developed calibrator for FastLec-Hepa will improve traceability and enable simultaneous assay and data storage in multiple diagnostic facilities. The data obtained with diluted serum samples demonstrated a high level of assay reproducibility and a very favorable linear detection range (**Supplementary Fig. 14**). Furthermore, we found an excellent agreement between assay values for serum and plasma prepared simultaneously from the same patient. Presently, we have about 10,000 sera and plasma available with detailed clinical notes collected in more than 10 facilities in Japan, and a series of retrospective studies is under way. We will shortly conclude licensing of our system for clinical implementation, based largely on the trials of the present study. In contrast to this, the majority of recent noninvasive techniques are currently shifting to physical measurements such as FibroScan, acoustic radiation force impulse[36] and real-time strain elastography[37]. Any on-site assay of large numbers of blood samples should provide a diagnostic value comparable to that of FibroTest, and a direct comparison in the same patient group will be necessary to evaluate this. We note here that according to a recent statistical validation method[38], predicted AUC of the diagnostic value of FibroTest for detection of advanced fibrosis in our sample set (DANA score = 1.81) was approximately 0.77, which was comparable to the AUC of FastLec-Hepa we obtained (0.79).

FastLec-Hepa has adopted a new paradigm for clinical diagnosis, "glyco-diagnosis", which is based on the quantity and quality of protein glycosylation patterns that well indicate disease progression. To detect such changes in glycosylation by conventional methods (e.g., mass spectrometry, liquid chromatography, or capillary electrophoresis), it is absolutely necessary to liberate the glycans of interest from their protein linkages[15,17,39]. It is possible to employ an alternative technology, which is based on a lectin–antibody sandwich immunodetection system for intact glycoproteins bearing disease-specific glyco-alterations. Such assays have been used to detect changes in fucosylation of *N*-linked glycans, which are associated with liver disease. However, in the present study, fucose-binding lectins were classified as "high noise" (**Fig. 2b**), and thus an enrichment of the target protein was the essential process in the assay. Lectin-overlay detection is performed typically after on-plate enrichment of the target glycoproteins by an immobilized antibody. In such cases, detection relies on a low avidity (high dissociation rate) between the captured glycoprotein and the overlaid lectin probe (see *right* of **Supplementary Fig. 3b**). These kinetic considerations essentially eliminate the use of an automated bedside clinical chemistry analyzer. Even though a fucose-binding lectin was immobilized on the beads (see *left* of **Supplementary Fig. 3b**), it still remains a problem for reliable quantitation by autoanalyzer. Our previous system LecT-Hepa[16,18,19,26], which detects the level of fucosylated α1-acid glycoprotein, requires enrichment of the protein prior to the assay.

In the present study, we have developed a strategy to overcome these problems in glyco-diagnosis associated with clinical implementation, and realized a rapid "on-site diagnosis" system (17 min, within the minimum time required for single assay by HISCL), based on analysis of a glycomarker (**Supplementary Fig. 1**). The strategy for selecting the most robust lectin led us to WFA, and away from the use of fucose-binding lectins, for the direct measurement system (**Fig. 2**). The diagnostic utility of M2BP, a protein resembling "sweet-doughnut"[20], brought a favorable density and orientation of the disease-related glycan on the homomultimer. These characteristic structures resulted in a major increase in the avidity of M2BP for the plated WFA. The resulting glycan–lectin interaction, which is remarkably strong and specific, made it possible to develop the rapid and highly sensitive assay (see *left* of **Supplementary Fig. 3b**). We believe that this unique strategy will revolutionize the use of glyco-diagnosis in clinical medicine and potentially provide a framework for the development of a new generation of biomarker assays.

## Methods

**Patient samples, biochemical parameters and indices.** Patients with chronic hepatitis were enrolled at Nagoya City University Hospital and Hokkaido University Hospital. Healthy volunteers as the controls were randomly selected in Nagoya City University Hospital (70 individuals) and AIST (48 individuals). The institutional ethics committees at Nagoya City University Hospital, Hokkaido University Hospital, and AIST approved this study, and informed consent for the use of their clinical specimens was obtained from all participants before the collection. In addition, we used 1,000 serum samples from virus-negative Caucasians as the normal population, which were purchased from Complex Antibodies Inc. (Fort Lauderdale, FL) and collected under IRB-approved collection protocols. Fibrosis was graded in the patients according to the histological activity index (HAI) using biopsy or surgical specimens. Biopsy specimens were classified as follows: F0, no fibrosis; F1, portal fibrosis without septa; F2, few septa; F3, numerous septa without cirrhosis; and F4, cirrhosis. The three diagnostic targets in this study were defined as significant fibrosis: F2+F3+F4; severe fibrosis: F3+F4; and cirrhosis: F4. Hepatic inflammation was also assessed according to the HAI, as follows: A0, no activity; A1, mild activity; A2, moderate activity; and A3, severe activity. Cirrhosis was confirmed by ultrasonography (coarse liver architecture, nodular liver surface, and blunt liver edges), evidence of hypersplenism (splenomegaly on ultrasonography) and/or a platelet count of $< 100{,}000/mm^3$. Virological responses during PEG-interferon-α and ribavirin therapy were defined as follows[5]: SVR, absence of HCV RNA from serum 24 weeks following discontinuation of therapy; nonresponder, failure to clear HCV RNA from serum after 24 weeks of therapy; relapse, reappearance of HCV RNA in serum after therapy was discontinued. For all patients, age and sex were recorded and serum levels of the following were analyzed: aspartate aminotransferase (AST), alanine aminotransferase (ALT), γ-glutamyltransferase (GGT), total bilirubin,

albumin, cholinesterase, total cholesterol, platelet count (PLT), hyaluronic acid (HA). The FIB-4 index was calculated as follows: [age (years) × AST (U/L)]/[platelets ($10^9$/L) × ALT (U/L)$^{1/2}$][26]. Fibrosis-specific glyco-alteration of α1-acid glycoprotein was determined by lectin–antibody sandwich immunoassays with a combination of three lectins (*Datura stramonium* agglutinin (DSA), *Maackia amurensis* leukoagglutinin (MAL), and *Aspergillus oryzae* lectin (AOL))[16]. All assays used an automated chemiluminescence enzyme immunoassay system (HISCL-2000i; Sysmex Co., Kobe, Japan)[18].

**Enrichment of M2BP from serum.** An automated protein purification system (ED-01; GP BioSciences Ltd., Yokohama, Japan) was used to immunoprecipitate M2BP from serum specimens. In brief, sera (2 μl) were diluted 10-fold with PBS/0.2%(w/v) SDS, heated at 95°C for 20 min, mixed with 10 μl of Triton X-100 in TBS (TBSTx) and injected into a 96-well SUMILON microtiter plate (Sumitomo Bakelite Co., Ltd., Tokyo, Japan). The plate and working reagents, including biotinylated anti-M2BP antibody (10 ng/μl), streptavidin-coated magnetic beads, washing buffer (1% TBSTx) and elution buffer (TBS containing 0.2% SDS), were loaded into the system. This generated 110 μl of purified M2BPs per serum sample (96 samples in 3.5 h).

**Western blot analysis.** Anti-human M2BP polyclonal antibody was purchased from R&D Systems, Inc. (Minneapolis, MN) and biotinylated with Biotin Labeling Kit – $NH_2$ (Dojindo Laboratories, Kumamoto, Japan). Purified serum M2BPs were electrophoresed under reducing conditions on 5–20% polyacrylamide gels (DRC, Tokyo, Japan) and transferred to PVDF membranes. After treatment with Block Ace® (DS Pharma Biomedical Co., Ltd., Osaka, Japan), the membranes were incubated with biotinylated anti-M2BP polyclonal antibody, and then with alkaline phosphatase-conjugated streptavidin (1/5000 diluted with TBST; ProZyme, Inc., San Leandro, CA). The membranes were incubated with Western Blue stabilized substrate for alkaline phosphatase (Promega, Madison, WI).

**Lectin microarray analysis.** Enriched M2BPs were analyzed with an antibody-overlay lectin microarray[24]. Purified protein (14 μl) was diluted to 60 μl with PBS containing 1%(v/v) Triton X-100 (PBSTx); this was applied to a LecChip™ (GP BioSciences Ltd.), which included three spots of 45 lectins in each of seven reaction wells. After incubation for 12 h at 20°C, 2 μl of human serum IgG (10 mg/ml) was added to the reaction solution on each chip and incubated for 30 min. The reaction solution was then discarded, and the chip was washed three times with PBSTx. Subsequently, 60 μl (200 ng) of biotinylated anti-human M2BP in PBSTx was applied to the chip, and incubated for 1 h. After three washes with PBSTx, 60 μl (400 ng) of a Cy3-labeled streptavidin (GE Healthcare, Buckinghamshire, UK) solution in PBSTx was added and incubated for 30 min. The chip was rinsed with PBSTx, scanned with an evanescent-field fluorescence scanner (GlycoStation™ Reader1200; GP BioSciences Ltd.) and analyzed with the Array Pro Analyzer software package, version 4.5 (Media Cybernetics, Inc., Bethesda, MD). The chip was scanned with the gain set to register a maximum net intensity < 40,000 for the most intense spots. The net intensity value for each spot was calculated by subtracting the background value from the signal intensity value. The relative intensity of lectin-positive samples was determined from the ratio of their fluorescence to the fluorescence of the internal-standard lectin, DSA.

**Quantitation of *Wisteria floribunda* agglutinin (WFA)-binding M2BP.** Serum was pretreated as described above under enrichment of M2BP from serum. Pretreated samples (50 μl) were diluted with an equal volume of starting buffer (0.1%(w/v) SDS in PBSTx), added to the WFA-coated agarose in a microtube (20 μl slurry; Vector Lab., Burlingame, UK), and incubated at 4°C for 5 h with gentle shaking. After centrifugation of the reaction solution at 2000 × *g* for 10 min, the supernatant was removed to a new microtube. The precipitate was suspended in 50 μl of the starting buffer, recentrifuged and this second supernatant combined with the first (designated as path-through fraction T). The precipitate was then washed with 200 μl of the starting buffer and the bound glycoproteins were eluted with 60 μl of 200 mM galactosamine/0.02%(w/v) SDS in PBS (designated as elution fraction E). M2BP was immunoprecipitated from fractions T and E and examined by electrophoresis under reducing conditions on 5–20% gradient SDS–polyacrylamide gels.

**WFA-antibody sandwich ELISA.** Flat-bottomed 96-well streptavidin-precoated microtiter plates (Nunc, Int., Tokyo, Japan) were treated with biotinylated WFA (Vector, 250 ng/well) for 1 h at room temperature. The plates were incubated with the diluted serum samples (50 μl) in PBS containing 0.1%(v/v) Tween20 (PBS-t) for 2 h at room temperature and then with 50 ng/well of the anti-human M2BP polyclonal antibody, in PBS-t for 2 h at room temperature. The plates were washed extensively and then incubated with 50 μl of horseradish peroxidase (HRP)-conjugated anti-mouse IgG (Jackson ImmunoResearch Laboratories Inc., Philadelphia, PA) at 1:10,000 in PBS-t for 1 h at room temperature. The substrate 3,3′,5,5′-tetramethylbenzidine (Thermo Fisher Scientific, Fremont, CA) solution (100 μl) was added to each well. The enzyme reaction was stopped by adding 100 μl of 1 M sulfuric acid, and the optical density measured at 450 nm.

**WFA-antibody sandwich immunoassay by HISCL.** The fibrosis-specific form of glycosylated M2BP was measured based on a sandwich immunoassay approach. Glycosylated M2BP was captured by WFA immobilized on magnetic beads, and the bound product was assayed with an anti-human M2BP monoclonal antibody linked to alkaline phosphatase (ALP-αM2BP). Two reagent packs (M2BP-WFA detection pack and a chemiluminescence substrate pack) were loaded in the HISCL. The detection pack comprised three reagents: a reaction buffer solution (R1), a WFA-coated magnetic beads solution (R2) and an ALP-αM2BP solution (R3). The chemiluminescence substrate reagent pack contained a CDP-Star substrate solution (R4) and a stopping solution (R5). Typically, serum (10 μl) was diluted to 60 μl with R1 and then mixed with R2 (30 μl). After the binding reaction, R3 (100 μl) was added to the reaction solution. The resultant conjugates were magnetically separated from unbound components, and mixed well with R4 (50 μl) and R5 (100 μl) before reading of the fluorescence. The chemiluminescent intensity was acquired within a period of 17 min in the operation described above. The reaction chamber was kept at 42°C throughout.

**Statistics.** Statistical analyses and graph preparation used Dr. SPSS II Windows software (SPSS Co., Tokyo, Japan), GraphPad Prism 5.0 (GraphPad Software Inc., La Jolla, CA), and Windows Excel 2007. This facilitated selection of the optimal lectin for analysis of fibrosis and a comparison of the diagnostic value of other serological fibrosis markers and indices. Because the data distribution for each parameter was non-Gaussian, the *P*-values were determined by nonparametric tests, such as the Mann–Whitney *U* test and Wilcoxon signed-rank test. Correlations with liver fibrosis were estimated as the significance of differences among the staging groups (F0–1, F2, F3, and F4) determined by Kruskal–Wallis nonparametric one-way analysis of variance. To assess classification efficiencies for detecting significant fibrosis, severe fibrosis and cirrhosis, the receiver-operating characteristic (ROC) curve analysis was also carried out to determine the area under the curve (AUC) values. Cutoff values obtained from Youden's index were used to classify patients. Diagnostic accuracy was expressed in terms of specificity, sensitivity and AUC.


1. "Nature Outlook Hepatitis C" edited by Brody, H. *et al. Nature* **474**, S1–S21 (2011).
2. Ge, D. *et al.* Genetic variation in IL28B predicts hepatitis C treatment-induced viral clearance. *Nature* **461**, 399–401 (2009).
3. Suppiah, V. *et al.* IL28B is associated with response to chronic hepatitis C interferon-alpha and ribavirin therapy. *Nat. Genet.* **41**, 1100–1104 (2009).
4. Tanaka, Y. *et al.* Genome-wide association of IL28B with response to pegylated interferon-alpha and ribavirin therapy for chronic hepatitis C. *Nat. Genet.* **41**, 1105–1109 (2009).
5. Ghany, M. G., Strader, D. B., Thomas, D. L. & Seeff, L. B. Diagnosis, management, and treatment of hepatitis C: an update. *Hepatology* **49**, 1335–1374 (2009).
6. Afdhal, N. H. *et al.* hepatitis C pharmacogenetics: state of the art in 2010. *Hepatology* **53**, 336–345 (2011).
7. Peng, C. Y., Chien R. N. & Liaw, Y. N. Hepatitis B virus-related decompensated liver cirrhosis: benefits of antiviral therapy. *J. Hepatol.* **57**, 442–450 (2012).
8. Chang, T. T. *et al.* Long-term entecavir therapy results in the reversal of fibrosis/cirrhosis and continued histological improvement in patients with chronic hepatitis B. *Hepatology* **52**, 886–893 (2010).
9. Shiratori, Y. *et al.* Histologic improvement of fibrosis in patients with hepatitis C who have sustained response to interferon therapy. *Ann. Intern. Med.* **132**, 517–524 (2000).
10. Castera, L. Non-invasive assessment of liver fibrosis in chronic hepatitis C. *Hepatol. Int.* **5**, 625–634 (2011).
11. Imbert-Bismut, F. *et al.* Biochemical markers of liver fibrosis in patients with hepatitis C virus infection: a prospective study. *Lancet* **357**, 1069–1075 (2001).
12. Calès, P. *et al.* A novel panel of blood markers to assess the degree of liver fibrosis. *Hepatology* **42**, 1373–1381 (2005).
13. Castera, L. *et al.* Prospective comparison of two algorithms combining non-invasive methods for staging liver fibrosis. *J. Hepatol.* **52**, 191–198 (2010).
14. Boursier, J. *et al.* Comparison of eight diagnostic algorithm for liver fibrosis in hepatitis C: new algorithms are more precise and entirely noninvasive. *Hepatology* **55**, 58–67 (2012).
15. Callewaert, N. *et al.* Noninvasive diagnosis of liver cirrhosis using DNA sequencer-based total serum protein glycomics. *Nat. Med.* **10**, 429–434 (2004).
16. Kuno, A. *et al.* Multilectin assay for detecting fibrosis-specific glyco-alteration by means of lectin microarray. *Clin. Chem.* **57**, 48–56 (2011).
17. Vanderschaeghe, D. *et al.* High-throughput profiling of the serum N-glycome on capillary electrophoresis microfluidics systems: toward clinical implementation of GlycoHepatoTest. *Anal. Chem.* **82**, 7408–7415 (2010).
18. Kuno, A. *et al.* LecT-Hepa: A triplex lectin-antibody sandwich immunoassay for estimating the progression dynamics of liver fibrosis assisted by a bedside clinical chemistry analyzer and an automated pretreatment machine. *Clin. Chim. Acta* **412**, 1767–1772 (2011).
19. Du, D. *et al.* Comparison of LecT-Hepa and FibroScan for assessment of liver fibrosis in hepatitis B virus infected patients with different ALT levels. *Clin. Chim. Acta* **413**, 1796–1799 (2012).
20. Sasaki, T., Brakebusch, C., Engel, J. & Timpl, R. Mac-2 binding protein is a cell-adhesive protein of the extracellular matrix which self-assembles into ring-like structures and binds beta1 integrins, collagens and fibronectin. *EMBO J.* **17**, 1606–1613 (1998).
21. Iacovazzi, P. A. *et al.* Serum 90K/MAC-2BP glycoprotein in patients with liver cirrhosis and hepatocellular carcinoma: a comparison with alpha-fetoprotein. *Clin. Chem. Lab. Med.* **39**, 961–965 (2001).

22. Artini, M. *et al.* Elevated serum levels of 90K/MAC-2 BP predict unresponsiveness to alpha-interferon therapy in chronic HCV hepatitis patients. *J. Hepatol.* **25**, 212–217 (1996).
23. Cheung, K. J. *et al.* The HCV serum proteome: a search for fibrosis protein markers. *J. Viral. Hepat.* **16**, 418–429 (2009).
24. Kuno, A. *et al.* Focused differential glycan analysis with the platform antibody-assisted lectin profiling for glycan-related biomarker verification. *Mol. Cell. Proteomics* **8**, 99–108 (2008).
25. Kuno, A. *et al.* Evanescent-field fluorescence-assisted lectin microarray: a new strategy for glycan profiling. *Nat. Met.* **2**, 851–856 (2005).
26. Vallet-Pichard, A. *et al.* FIB-4: an inexpensive and accurate marker of fibrosis in HCV infection. Comparison with liver biopsy and fibrotest. *Hepatology* **46**, 32–36 (2007).
27. Ito, K. *et al.* LecT-Hepa, a glyco-marker derived from multiple lectins, as a predictor of liver fibrosis in chronic hepatitis C patients. *Hepatology* **56**, 1448–1456 (2012).
28. Bruno, S. *et al.* Sustained virological response to interferon-α is associated with improved outcome in HCV-related cirrhosis: A retrospective study. *Hepatology* **45**, 579–587 (2007).
29. Cardoso, A.-C. *et al.* Impact of peginterferon and ribavirin therapy on hepatocellular carcinoma: Incidence and survival in hepatitis C patients with advanced fibrosis. *J. Hepatol.* **52**, 652–657 (2010).
30. Morgan, T. R. *et al.* Outcome of sustained virological responders with histologically advanced chronic hepatitis C. *Hepatology* **52**, 833–844 (2010).
31. Lupberger, J. *et al.* EGFR and EphA2 are host factors for hepatitis C virus entry and possible targets for antiviral therapy. *Nat. Med.* **17**, 589–595 (2011).
32. Iwasaki, Y. *et al.* Risk factors for hepatocellular carcinoma in hepatitis C patients with sustained virologic response to interferon therapy. *Liver Int.* **24**, 603–610 (2004).
33. Ikeda, K. *et al.* Anticarcinogenic impact of interferon on patients with chronic hepatitis C: A large-scale long-term study in a single center. *Intervirology* **49**, 82–90 (2006).
34. Kurosaki, M. *et al.* Data mining model using simple and readily available factors could identify patients at high risk for hepatocellular carcinoma in chronic hepatitis C. *J. Hepatol.* **56**, 602–608 (2012).
35. Schuppan, D. & Pinzani, M. Anti-fibrotic therapy: lost in translation? *J. Hepatolol.* **56**, S66–74 (2012).
36. Rizzo, L. *et al.* Comparison of transient elastography and acoustic radiation force impulse for non-invasive staging of liver fibrosis in patients with chronic hepatitis C. *Am. J. Gastroenterol.* **106**, 2112-2120 (2011).
37. Ferraioli, G. *et al.* Performance of real-time sitrain elastography, transient elastgraphy, and aspartate-to-platelet ration index in the assessment of fibrosis in chronic hepatitis C. *AJR Am. J. Roentgenol.* **199**, 19–25 (2012).
38. Poynard, T. *et al.* Standardization of ROC curve areas for diagnostic evaluation of liver fibrosis markers based on prevalences of fibrosis stages. *Clin. Chem.* **53**, 1615–1622 (2007).
39. Nishimura, S. Toward automated glycan analysis. *Adv. Carbohydr. Chem. Biochem.* **65**, 219–271 (2011).


## Acknowledgments

This work was supported in part by a grant from New Energy and Industrial Technology Development Organization of Japan. We thank H. Ozaki, H. Shimazaki, S. Unno, K. Saito, M. Sogabe, Y. Kubo, J. Murakami, S. Shirakawa, T. Fukuda (AIST), and H. Naganuma (NCU) for technical assistance. We also thank A. Togayachi, T. Sato, H. Kaji, J. Hirabayashi, H. Tateno, A. Takahashi (AIST) and C. Tsuruno, S. Nagai and Y. Takahama (Sysmex Co.) for critical discussion.

## Author contributions:

A.K. conceived and designed the study, performed most of the biochemical experiments, analyzed data and wrote the paper with comments from Y.T., M.M. and H.N.; Y.I. conceived and designed the study, performed the sample pre-treatment for the assay, and analyzed data; Y.T., K.I., M.M., and S.H collected clinical samples, designed the validation study, and analyzed data; A.M. and S.S. performed the biochemical experiments including lectin microarray analysis and analyzed data; M.S. and M.K. performed staging of biopsy specimens by histological activity index (HAI); H.N. conceived and designed the study, and supervised all aspects of the work; and all authors discussed the results and implications, and commented on the paper.

## Additional information

**Supplementary information** accompanies this paper at http://www.nature.com/scientificreports

**Competing financial interests:** The authors declare no competing financial interests.



**How to cite this article:** Kuno, A. *et al.* A serum "sweet-doughnut" protein facilitates fibrosis evaluation and therapy assessment in patients with viral hepatitis. *Sci. Rep.* **3**, 1065; DOI:10.1038/srep01065 (2013).

Bioorganic & Medicinal Chemistry Letters 23 (2013) 503–506

Contents lists available at SciVerse ScienceDirect

Bioorganic & Medicinal Chemistry Letters

journal homepage: www.elsevier.com/locate/bmcl

# 2′-Fluoro-6′-methylene-carbocyclic adenosine phosphoramidate (FMCAP) prodrug: In vitro anti-HBV activity against the lamivudine–entecavir resistant triple mutant and its mechanism of action

Ravindra K. Rawal [a], Uma S. Singh [a], Satish N Chavre [a], Jianing Wang [a], Masaya Sugiyama [b], Wai Hung [a], Rajgopal Govindarajan [a], Brent Korba [c], Yasuhito Tanaka [b], Chung K. Chu [a,*]

[a] The University of Georgia, College of Pharmacy, Athens, GA 30602, USA
[b] Nagoya City University Graduate School of Medical Sciences, Nagoya 467 8601, Japan
[c] Georgetown University Medical Center, WA 20057, USA

ARTICLE INFO

*Article history:*
Received 28 September 2012
Accepted 8 November 2012
Available online 24 November 2012

*Keywords:*
Carbocyclic-nucleos(t)ide
Anti-HBV activity
Wild-type
Lamivudine–entecavir triple mutant
Drug-resistant mutants

ABSTRACT

Novel 2′-fluoro-6′-methylene-carbocyclic adenosine (FMCA) monophosphate prodrug (FMCAP) was synthesized and evaluated for its in vitro anti-HBV potency against a lamivudine–entecavir resistant clone (L180M + M204V + S202G). FMCA demonstrated significant antiviral activity against wild-type as well as lamivudine–entecavir resistant triple mutant (L180M + M204V + S202G). The monophosphate prodrug (FMCAP) demonstrated greater than 12-fold (12×) increase in anti-HBV activity without increased cellular toxicity. Mitochondrial and cellular toxicity studies of FMCA indicated that there is no significant toxicity up to 100 μM. Mode of action studies by molecular modeling indicate that the 2′-fluoro moiety by hydrogen bond as well as the Van der Waals interaction of the carbocyclic ring with the phenylalanine moiety of the polymerase promote the positive binding, even in the drug-resistant mutants.



The chronic HBV infection is strongly associated with liver diseases like chronic hepatic insufficiency, cirrhosis and hepatocellular carcinoma (HCC).[1] According to the World Health Organization (WHO), currently about 2 billion people world-wide have been infected with HBV and more than 350 million live with chronic infection. Acute or chronic outcomes of HBV infection are estimated to cause the deaths of 600,000 people worldwide every year.[2]

Currently, there are several nucleos(t)ide analogues available to treat chronic hepatitis B virus infection.[3–6] The major target of these drugs is to inhibit the viral reverse transcriptase (RT)/DNA polymerase, which is responsible for the synthesis of the minus-strand DNA. Although the currently used agents are well tolerated and effective in suppressing the viral replication for extended periods, the significant rate of virological relapse caused by drug resistance remains a critical issue.

Lamivudine (LVD) was first introduced as the orally active anti-HBV agent in 1998. Lamivudine profoundly suppresses HBV replication in patients with chronic hepatitis B infection; however, lamivudine-resistant HBV (LVDr) was isolated from a significant numbers of patients during the treatment with lamivudine. Currently, there are several antiviral options exist for these patients viz., to use adefovir or high dose (1.0 mg/day) of entecavir, or more recently tenofovir. However, this resulted in also the development of resistance mutants during the long term therapy. At present, entecavir is the most prescribed drug, and is recommended for patients with the wild-type as well as for those harboring adefovir and lamivudine-resistant strains. However, recent clinical studies by Tanaka and his co-workers suggested that the entecavir mutant in the lamivudine-resistant patients (L180M + M204V + S202G) causes a viral breakthrough: 4.9% of patients at baseline increases to 14.6%, 24% and 44.8% at weeks 48, 96 and 144, respectively.[7] Therefore, it is of great interest to discover novel anti-HBV agent, which is effective against lamivudine- and entecavir-resistant triple mutants (L180M + M204V + S202G).

The potency of a nucleos(t)ide analogue is determined by its ability to serve as a competitive inhibitor of the HBV polymerase relative to that of the natural substrate, the nucleotide triphosphate.[8] However, host cellular kinases limit the pharmacological potency of nucleoside analogues by phosphorylation to their corresponding triphosphates. Particularly, the initial kinase action on the nucleoside to the monophosphate is the rate-limiting step. However, many synthetic nucleosides are not phosphorylated or the rate of phosphorylation is very slow due to the structural requirement of the kinases, resulting in only generating a low quantity of the triphosphate. To overcome this phosphorylation issue, nucleoside phosphoramidate prodrugs have been introduced,[8,9] which

* Corresponding author. Address: Department of Pharmaceutical and Biomedical Sciences, College of Pharmacy, The University of Georgia, Athens, GA 30602, USA. Tel.: +1 706 542 5379; fax: +1 706 542 5381.
*E-mail address:* DCHU@rx.uga.edu (C.K. Chu).

0960-894X/$ - see front matter © 2012 Elsevier Ltd. All rights reserved.
http://dx.doi.org/10.1016/j.bmcl.2012.11.027

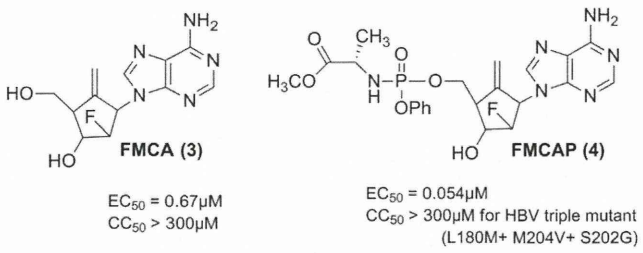


**Figure 1.** Structures of 2′-fluoro-6′-methylene-carbocyclic adenosine (FMCA; **3**) and its prodrug (FMCAP; **4**).

can bypass the rate-limiting first step of monophosphorylation. Phosphoramidate prodrugs have demonstrated to enhance the nucleoside potency in cell culture as well as in patients.[10,11] This methodology greatly increases the lipophilicity of the nucleotide to increase the cell penetration as well as to target the liver cells in vivo.

In this communication, we present that a FMCA phosphoramidate prodrug is such an agent, which can potentially be used for the treatment of patients who experience viral breakthrough due to the triple mutants caused by the use of lamivudine and entecavir.

In our previous report, we have demonstrated that the novel carbocyclic adenosine analog **3** (FMCA Fig. 1) exhibits significant anti-HBV activity against wild type as well as adefovir/lamivudine resistant strains.[12] The present study describes the synthesis and antiviral evaluation of a phosphoramidate of FMCA (FMCAP), which demonstrated the significantly improved in vitro potency. Additionally, we studied its mechanism of action how FMCA-TP can effectively bind to the HBV polymerase by molecular modeling and still exerts the antiviral activity against the lamivudine–entecavir triple mutant (L180M + M204V + S202G).

FMCAP (**4**, Scheme 1)[13] was synthesized using a known method in the literature,[14,15] in which the phosphorylation of phenol with phosphorus oxychloride generates phenyl dichlorophosphate **1**, which was coupled with L-alanine methyl ester in the presence of *tri*-ethyl amine in dichloromethane to give chlorophosphoramidate reagent **2**, which, in turn, was coupled with FMCA **3** in the presence of 1-methyl imidazole in THF to furnish the phosphoramidate **4** in good yield.

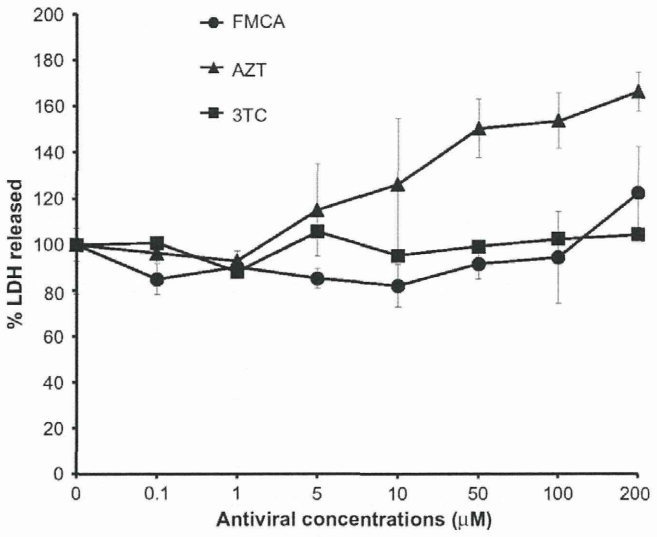


**Figure 2.** Mitochondrial toxicity of FMCA **3**, AZT and 3TC through lactate dehydrogenase release (LDH) assay.

FMCA **3** and FMCAP **4** were evaluated in vitro against the wild-type as well as the lamivudine–entecavir resistant clone (L180M + S202I + M202V). The FMCA **3** and FMCAP **4** demonstrated significant anti-HBV activity ($EC_{50}$ 0.548 ± 0.056 & 0.062 ± 0.011 μM, respectively) against the wild-type virus, while lamivudine and entecavir also demonstrated potent anti-HBV activity ($EC_{50}$ 0.056 ± 0.003 & 0.008 μM, respectively) (Table 1). It is noteworthy to mention that the anti-HBV potency of FMCAP (**4**) was increased to eight-fold (8×) in comparison to that of FMCA **3**, which indicates the importance of the initial phosphorylation of the nucleoside.

FMCA **3** and FMCAP **4** were further evaluated for their in-vitro antiviral potency against a lamivudine–entecavir resistant clone (L180M + M204V + S202G). It was observed that the anti-HBV potency of both FMCA **3** and FMCAP **4** ($EC_{50}$ 0.67 & 0.054 μM, respectively) were maintained against the resistant clone, and furthermore, the anti-HBV activity of FMCAP **4** was enhanced a 12-fold (12×) with respect to that of FMCA without significant enhancement of cellular toxicity. It was also noteworthy to mention that the anti-HBV potency of entecavir against the mutant

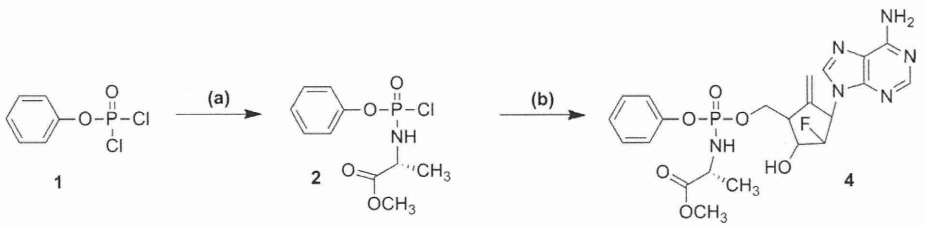


**Scheme 1.** Reagent and conditions: (a) L-alanine methyl ester hydrochloride, $Et_3N$, $CH_2Cl_2$; (b) FMCA (3), NMI, THF, rt overnight.

**Table 1**
In vitro anti-HBV activity of FMCA **3**, FMCAP **4**, lamivudine and entecavir against wild-type and entecavir drug-resistant mutant (L180M + M204V + S202G) in Huh7 cells

| Compounds | HBV Strains | | | |
|---|---|---|---|---|
| | Wild-type | | | L180M + M204V + S202G |
| | $EC_{50}$ (μM) | $EC_{90}$ (μM) | $CC_{50}$ (μM) | $EC_{50}$ (μM) |
| FMCA **3** | 0.548 ± 0.056 | 6.0 ± 0.400 | >300 | 0.67 |
| FMCAP **4** | 0.062 ± 0.011 | 0.46 ± 0.060 | >300 | 0.054 |
| Lamivudine | 0.056 ± 0.003 | 0.142 ± 0.008 | >300 | >500[17] |
| Entecavir | 0.008 | 0.033 | 28 | 1.20[16] |

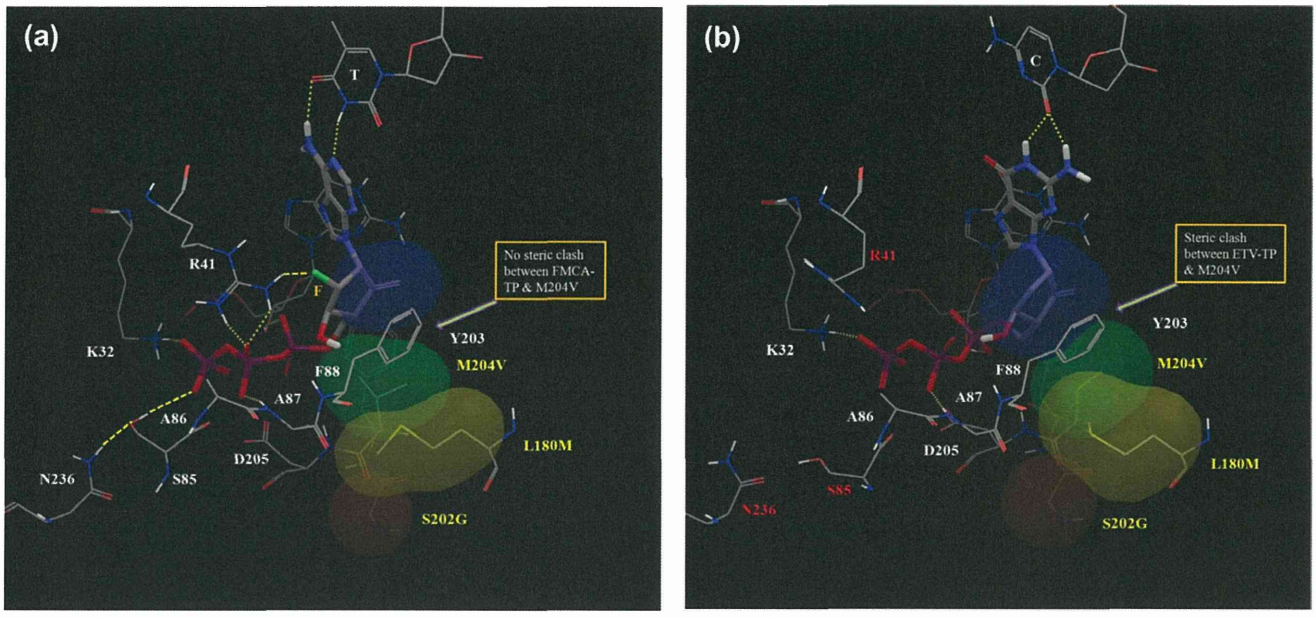


**Figure 3.** (a) FMCA-TP binding mode in ETVr (L180M + M204V + S202G); and (b) ETV-TP binding mode in ETVr (L180M + M204V + S202G) and there is a steric hindrance. Yellow dotted lines are hydrogen bonding interactions (<2.5 Å). The Van der Waals surface of L180M is colored yellow. The Van der Waals surface of M204V is shown in spring green. The Van der Waals surface of S202G is colored orange. The exocyclic double bond is shown blue color.

**Table 2**
MBAE (multi-ligand bimolecular association with energetics) calculation of FMCA-TP and ETV-TP after Glide XP docking[21] and energy minimization[22]

| Strains | Compounds | Energy difference results (ΔE, kcal/mol) | | |
|---|---|---|---|---|
| | | Total energy | VdW[a] | Electrostatic |
| Wild-type | FMCA-TP | −588.05 | 375.78 | −6341.08 |
| | ETV-TP | −597.25 | 350.35 | −6009.65 |
| ETVr | FMCA-TP | −591.54 | 359.91 | −6245.68 |
| (L180M + M204V + S202G) | ETV-TP | −320.28 | 248.82 | −4831.12 |

[a] Van der Waals interaction.

was reduced by 150-fold ($EC_{50}$ 1.2 μM) in comparison to wild type.[16]

In the preliminary mitochondrial toxicity studies in HepG2 cells by measuring the lactic dehydrogenase release,[18] FMCA **3** did not exhibit any significant toxicity up to 100 μM like lamivudine (3TC), while azidothymidine (AZT) shows the increase of toxicity (Fig. 2).

In our previous report, we described molecular modeling studies for favorable anti-HBV activity of FMCA-TP in wild-type as well as in N236T adefovir resistant (ADVr) mutant.[12] In the current studies, it was of interest to know how the FMCA and its prodrug maintain the anti-HBV activity against ETVr triple mutant (L180M + M204V + S202G) in comparison to entecavir. Therefore, molecular modeling studies were conducted to obtain the insight of the molecular mechanism of FMCA-TP by using the Schrodinger Suite modules.[19] A previously described homology model was used to further explore the impact of the ETVr to the HBV-RT.[12] The homology model of HBV-RT was constructed based on the published X-ray crystal structure of HIV reverse transcriptase (PDB code: 1RTD).[20]

The binding mode of FMCA-TP and ETV-TP in ETVr (L180M + M204V + S202G) HBV-RT are depicted in Figure 3a and b, respectively. Their MBAE (multi-ligand biomolecular association with energetics)[22] calculations of FMCA-TP (total energy, wt −588.05 & ETVr −591.54 kcal/mol) and ETV-TP (total energy, wt −597.25 & ETVr −320.28 kcal/mol) after glide XP (extra precision) docking[21] and energy minimization in ETVr HBV-RT are shown in Table 2. The triphosphate of FMCA-TP forms all the network of hydrogen bonds with the active site residues (Fig. 3a), K32, R41, S85 & A87 in the similar manner as in wild-type,[12] whereas ETV-TP lose the hydrogen bonding with R41 & S85. The γ-phosphate of FMCA-TP maintains a critical H-bonding with the OH of S85 with connection of hydrogen bonds between S85 and N236 in ETVr HBV-RT also. However, γ-phosphate ETV-TP does not maintain this critical H-bonding with S85 and N236 (Fig. 3b).

The carbocyclic ring with an exocyclic double bond of FMCA-TP and ETV-TP makes the favorable Van der Waals interaction with F88 in ETVr HBV-RT (Fig. 3a and b). There is no steric clash in between exocyclic double bond of FMCA-TP and M204V residue, whereas ETV-TP exocyclic double bond has steric clash with M204V residue in ETVr HBV-RT. The 2′-fluorine substituent in the carbocyclic ring of FMCA-TP appears to promote an additional binding with the NH of R41 guanidino group as shown in Figure 3a, which is in agreement with the antiviral activity of FMCA-TP shown in Table 1. Overall, the modeling studies can qualitatively explain the favorable anti-HBV activity of FMCA-TP against ETVr mutant (L180M + M204V + S202G) in comparison to entecavir as shown in Table 1.

In conclusion, 2′-fluoro-6′-methylene-carbocyclic adenosine phosphoramidate prodrug (FMCAP) was synthesized, which demonstrated the significantly increased anti-HBV potency relative to the parent compound, FMCA in vitro. Molecular modeling studies delineated the mechanism of FMCA-TP and how it can effectively bind to the lamivudine–entecavir resistant triple mutant resulting

in maintaining the anti-HBV activity against the mutant. Furthermore, FMCA has been studied for the release of lactic dehydrogenase for potential mitochondrial toxicity and found that no significant increase of toxicity of FMCA compared with other commonly used anti-HIV nucleoside drugs. Very recently, a preliminary in vivo study in chimeric mice harboring the triple mutant, FMCAP was found to reduce HBV viral load while entecavir did not (data not shown). In view of these promising anti-HBV activities and non-toxicity of FMCAP as well as the interesting mechanism of antiviral activity, the chiral synthesis of FMCAP and its mitochondrial toxicity studies for preclinical investigation are warranted.

## Acknowledgment

This research was supported by the U.S. Public Health Service Grant AI-25899 (C.K.C.), NOI-AI-30046 (B.K.) from the National Institute of Allergy and Infectious Diseases, NIH.

## References and notes

1. El-Serag, H. B. *N. Engl. J. Med.* **2011**, *365*, 1118.
2. http://www.who.int/mediacentre/factsheets/fs204/en/.
3. Sharon, A.; Jha, A. K.; Chu, C. K. *Analogue-Based Drug Discovery II*, 383.
4. Jarvis, B.; Faulds, D. *Drugs* **1999**, *58*, 101.
5. Marcellin, P.; Chang, T.; Lim, S. G.; Tong, M. J.; Sievert, W.; Shiffman, M. L.; Jeffers, L.; Goodman, Z.; Wulfsohn, M. S.; Xiong, S.; Fry, J.; Brosgart, C. L. *N. Engl. J. Med.* **2003**, *348*, 808.
6. Pol, S.; Lampertico, P. *J. Viral Hepat.* **2012**, *19*, 377.
7. Mukaide, M.; Tanaka, Y.; Shin, T.; Yuen, M. F.; Kurbanov, F.; Yokosuka, O.; Sata, M.; Karino, Y.; Yamada, G.; Sakaguchi, K. *Antimicrob. Agents Chemother.* **2010**, *54*, 882.
8. Hecker, S. J.; Erion, M. D. *J. Med. Chem.* **2008**, *51*, 2328.
9. Sofia, M. J.; Bao, D.; Chang, W.; Du, J.; Nagarathnam, D.; Rachakonda, S.; Reddy, P. G.; Ross, B. S.; Wang, P.; Zhang, H.-R.; Bansal, S.; Espiritu, C.; Keilman, M.; Lam, A. M.; Steuer, H. M. M.; Niu, C.; Otto, M. J.; Furman, P. A. *J. Med. Chem.* **2010**, *53*, 7202.
10. Chang, W.; Bao, D.; Chun, B.-K.; Naduthambi, D.; Nagarathnam, D.; Rachakonda, S.; Reddy, P. G.; Ross, B. S.; Zhang, H.-R.; Bansal, S.; Espiritu, C. L.; Keilman, M.; Lam, A. M.; Niu, C.; Steuer, H. M.; Furman, P. A.; Otto, M. J.; Sofia, M. J. *ACS Med. Chem. Lett.* **2010**, *2*, 130.
11. McGuigan, C.; Gilles, A.; Madela, K.; Aljarah, M.; Holl, S.; Jones, S.; Vernachio, J.; Hutchins, J.; Ames, B.; Bryant, K. D.; Gorovits, E.; Ganguly, B.; Hunley, D.; Hall, A.; Kolykhalov, A.; Liu, Y.; Muhammad, J.; Raja, N.; Walters, R.; Wang, J.; Chamberlain, S.; Henson, G. *J. Med. Chem.* **2010**, *53*, 4949.
12. Wang, J.; Singh, U. S.; Rawal, R. K.; Sugiyama, M.; Yoo, J.; Jha, A. K.; Scroggin, M.; Huang, Z.; Murray, M. G.; Govindarajan, R. *Bioorg. Med. Chem. Lett.* **2011**, *21*, 6328.
13. *Compound* **4**: $^{1}$H NMR (500 Mz, $CDCl_3$) $\delta$ 8.35 (s, 1H), 7.86 (d, $J$ = 3.0 Hz, 1H), 7.34–7.15 (m, 5H), 5.95 (m, 3H), 5.26 (d, $J$ = 8.0 Hz, 1H), 5.01–4.90 (m, 1H), 4.83 (s, 1H), 4.50–4.41 (m, 2H), 4.25–4.04 (m, 3H), 3.71 (s, 3H), 3.07 (s, 1H), 1.40 (d, $J$ = 6.5 Hz, 3 H); $^{19}$F NMR (500 MHz, $CDCl_3$) $\delta$ −192.86 (m, 1F); $^{13}$C NMR (125 MHz, $CDCl_3$) $\delta$ 171, 159.0, 156.5, 152.5, 150.4, 142.9, 130.1, 121.2, 120.3, 106.7, 102.4, 72.2, 71.1, 62.3, 51.9, 46.3, 43.9, 19.1; $^{31}$P NMR (202 MHz, $CDCl_3$): $\delta$ 2.67, 2.99. Anal. Calcd For $C_{22}H_{26}FN_6O_6P.0.5H_2O$: C, 49.91; H, 5.14; N, 15.87; Found C, 49.84; H, 5.06; N, 15.22.
14. McGuigan, C.; Pathirana, R. N.; Mahmood, N.; Devine, K. G.; Hay, A. J. *Antiviral Res.* **1992**, *17*, 311.
15. Liang, Y.; Narayanasamy, J.; Schinazi, R. F.; Chu, C. K. *Bioorg. Med. Chem.* **2006**, *14*, 2178.
16. Walsh, A. W.; Langley, D. R.; Colonno, R. J.; Tenney, D. J. *PloS one* **2010**, *5*, e9195.
17. Villet, S.; Ollivet, A.; Pichoud, C.; Barraud, L.; Villeneuve, J. P.; Trépo, C.; Zoulim, F. *J. Hepatol.* **2007**, *46*, 531.
18. Lai, Y.; Tse, C. M.; Unadkat, J. D. *J. Biol. Chem.* **2004**, *279*, 4490.
19. Schrodinger Suite 2012; LLC, NY, 2012.
20. http://www.rcsb.org/pdb.
21. Glide version 5.8; Schrodinger LLC, NY, 2012.
22. Macromodel version 9.9; Schrodinger LLC, NY, 2012.

肝臓　53巻1号　35-41（2012）


＜症例報告＞

# 多剤耐性変異を認めた悪性リンパ腫合併B型慢性肝炎に対しテノフォビルが著効した一例

渡邊　綱正[1)]　菅内　文中[2)]　楠本　茂[3)]　新海　登[4)]　飯尾　悦子[1)4)]
松浦健太郎[4)]　日下部篤宣[4)]　宮木　知克[4)]　野尻　俊輔[4)]　田中　靖人[1)*]

要旨：症例は33歳男性．B型肝炎無症候性キャリアの経過観察中に悪性リンパ腫を発症し，2001年よりラミブジン（LVD）投与が開始された．2005年にbreakthrough hepatitisを発症し，アデフォビル（ADV）追加併用療法に移行した．2007年にはエンテカビル（ETV）単独治療へ変更された．2008年，2回目のbreakthrough hepatitisと悪性リンパ腫の再発を認め，再度LVD＋ADV併用療法に変更した．しかし，ALT上昇とウイルス量高値が持続したため，耐性検査が実施された．L80I，L180M，A181T，T184I，M204I/Vの変異を確認し，多剤耐性変異と判断した．倫理委員会承認のもと，テノフォビル（TDF）＋LVD併用療法を開始し，ウイルス量の低下と肝炎の改善が得られた．合併する悪性リンパ腫に対して，化学療法後にB型肝炎キャリアである実兄から同種骨髄移植を施行した．移植後ドナー由来の野生株によるウイルス血症を呈したが，治療継続により改善した．今回，多剤耐性変異株，かつドナー由来の野生株ウイルスに対し，TDFが著効した症例を経験したため報告する．

索引用語：　テノフォビル　多剤耐性変異　breakthrough hepatitis
B型慢性肝炎　同種骨髄移植

## はじめに

厚生労働省研究班が定めた平成23年度のB型肝炎治療ガイドラインによれば，35歳未満はdrug freeを目指すIFNを中心とした治療を基本とし，35歳以上ではHBV DNAの持続的陰性化およびALT値の持続正常化を目指した核酸アナログ製剤の長期投与が基本となっている．さらに，HBe抗原の有無とHBV DNA量により，治療薬と治療期間の細分化を推奨している．わが国でB型肝炎治療に保険認可されている核酸アナログ製剤は，2000年に登場したラミブジン（lamivudine；LVD）[1)2)]，2004年のアデフォビル（adefovir dipivoxil；ADV）[3)4)]，2006年にエンテカビル（entecavir；ETV）[5)6)]が使用可能である．現在，核酸アナログ未使用例での第1選択薬はETVが推奨され，今後の耐性変異出現は少数例と予測されるが[7)]，これまでのLVD使用例やLVD耐性変異出現に対するADV併用例も少なくない．今後は，これら各種核酸アナログ製剤の使用期間の長期化に伴い，多剤耐性ウイルスの出現が懸念される．

我々は，B型肝炎を合併した悪性リンパ腫の治療経過中に，肝機能増悪と悪性リンパ腫の再発を呈し，早急なB型肝炎ウイルス（HBV）コントロールを必要とする症例を経験した．耐性ウイルス検査の結果，LVD，ADV，ETVのいずれの薬剤にも耐性を有した多剤耐性株によるbreakthrough hepatitis（BTH）であったため，テノフォビル（tenofovir disoproxil fumarate；TDF）を用いたrescue療法を施行した．多剤耐性HBVに対してTDFが奏功し，再発性悪性リンパ腫に対する全身化学療法およびHBVキャリアをドナーとする同種骨髄移植が安全に施行できた1例を経験したので，HBV DNA塩基配列の解析を加えて報告する．

1）名古屋市立大学大学院医学研究科病態医科学
2）名古屋市厚生院附属病院消化器内科
3）名古屋市立大学大学院医学研究科腫瘍・免疫内科学
4）名古屋市立大学大学院医学研究科消化器・代謝内科学
*Corresponding author: ytanaka@med.nagoya-cu.ac.jp
＜受付日2011年8月22日＞＜採択日2011年11月28日＞

**Table 1** Laboratory data on admission

| | | | | | |
|---|---|---|---|---|---|
| <CBC> | | <Blood chemistry> | | <Virus markers> | |
| WBC | 3590 /μl | TP | 6.8 g/dl | HBsAg | 14000 COI |
| Neut | 59 % | Alb | 4.2 g/dl | (CLIA) | |
| Ly | 31 % | T-Bil | 0.5 mg/dl | HBsAb | 0.5 mIU/ml |
| Mo | 10 % | D-Bil | 0.2 mg/dl | HBeAg | 256 COI |
| Eo | 1 % | AST | 82 IU/L | HBeAb | 0.1 % |
| Ba | 0 % | ALT | 122 IU/L | HBcAb | 100 % |
| RBC | $441\times10^4$ /μl | LDH | 187 IU/L | HBV-DNA | 6.5 log copies/ml |
| Hb | 15.0 g/dl | ALP | 230 IU/L | (RTD-PCR) | |
| Hct | 43.1 % | γ-GTP | 49 IU/L | HBV Genotype | C |
| Plt | $20.3\times10^4$ /μl | Ch-E | 165 IU/L | (RFLP) | |
| | | BUN | 14 mg/dl | HBV precore | Wild type |
| <Coagulation> | | Creat | 0.7 mg/dl | (PCR-ELMA) | |
| PT | 83.7 % | AMY | 50 IU/L | HBV core promoter | Mutant type |
| PT-INR | 1.11 INR | T-Cho | 154 mg/dl | (PCR-ELMA) | |
| APTT | 91.1 % | TG | 69 mg/dl | HCV Ab 3rd | (−) |
| | | Na | 143 mEq/L | | |
| | | K | 3.7 mEq/L | <Immunology> | |
| | | CL | 105 mEq/L | IgG | 1026 mg/dl |
| | | CRP | 0.04 mg/dl | IgA | 256 mg/dl |
| | | | | IgM | 120 mg/dl |

## 症　例

患者：33歳，男性．

現病歴：20歳代にB型慢性肝炎（無症候性キャリア）と診断され，経過観察されていた．2000年に鼠径リンパ節腫脹をきっかけに悪性リンパ腫（ろ胞性リンパ腫）stage IV（節外病変として上咽頭と小腸浸潤あり）と診断された．HBV合併を考慮して化学療法は施行せず，腫瘍量の制御目的に脾臓への局所放射線照射（計28.8 Gy）が選択された．その後，2001年1月にLDHの再上昇を認め，左腋窩リンパ節からの再生検によりびまん性大細胞型B細胞性リンパ腫（diffuse large B-cell lymphoma：DLBCL）と診断された．B型慢性肝炎は無症候性であったが，2001年2月からLVD 100 mg/日を開始した後に，化学療法（CHO療法）及び自家末梢血幹細胞移植を施行し，DLBCLは寛解維持となった．以降もLVDを継続服用していたが，2005年4月にbreakthrough hepatitis（BTH）を発症し（この時点での耐性ウイルス検査は未施行），LVD継続投与のままにADV 10 mg/日を追加した．LVD＋ADV併用療法により肝炎は鎮静化し，良好なウイルスコントロールを得ていたが，新規核酸アナログ剤であるETVの登場に伴い，2007年9月にLVD＋ADV併用療法からETV 0.5 mg/日の単独投与に治療変更された．2008年5月に2回目のBTHを認め，さらに翌6月には急激なリンパ節腫大に伴う呼吸困難感が出現し，早急なHBVコントロールと再発DLBCLに対するサルベージ治療目的で当院紹介となった．

既往歴：22歳：アデノイド摘出術．

家族歴：母：B型慢性肝炎，兄：B型慢性肝炎（無症候性キャリア）．

生活歴：飲酒：なし，喫煙：なし．

入院時現症：身長170 cm，体重69 kg，血圧111/64 mmHg，脈拍81/分，意識清明，眼瞼結膜に貧血なし，眼球結膜に黄疸なし，左鎖骨上部から正中にかけて約5×3 cmの一塊となった弾性硬なリンパ節を触知．頸部呼吸狭窄音聴取せず（ただし前屈姿勢で呼吸困難感出現あり），心音・呼吸音正常，腹部平坦，軟，圧痛なし，肝脾触知せず，羽ばたき振戦なし．

来院時検査所見（**Table 1**）：（2008.6.23所見：LVD＋ADV併用療法前）血液検査にてAST 82 IU/L，ALT 122 IU/L，T-Bil上昇なく，PT 92.0％と肝予備能は保持されていた．CLIAによるHBs抗原14000 COI，HBe抗原陽性，HBV DNA 6.5 log copies/mlと血中ウイルス

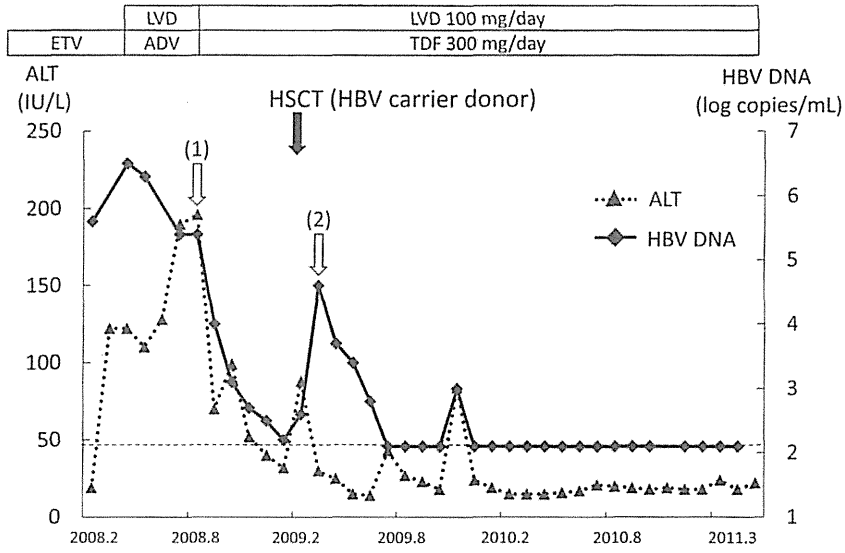


**Fig. 1** HBV viral load dynamics (black diamond shapes) and course of ALT (black triangles) during different treatment (ETV: entecavir; LVD: lamivudine; ADV: adefovir; TDF: tenofovir). HSCT: Hematopoietic stem cell transplantation. Hollow arrows indicate sampling times for HBV polymerase gene sequence analysis (see also Fig. 2)

**Table 2** Sequence mutations of prior TDF/LVD treatment regimens

| | rt A domain | rt B domain | | | | | | rt C domain | | rt D domain | rt E domain |
|---|---|---|---|---|---|---|---|---|---|---|---|
| | L80 | H169 | V173 | L180 | A181 | T184 | A194 | S202 | M204 | N236 | M250 |
| LVD | I | | L | M | | | | | I/V | | |
| ADF | | | | | T | | | | | T | |
| ETV | | T | | M | | I | | G/C | I/V | | I/V |
| TDF | | | | | | | T | | | | |

Gray areas indicated the existences of the mutations in this case.

量の増大を認めた．HBV precore（nt1896）/core promoter(nt1762/1764)はWild/Mutant typeであり，Genotypeはであった．

来院後経過（**Fig. 1**）：経過よりETV耐性株出現によるBTHを疑い，ETV単独投与から再度LVD 100 mg/日＋ADV 10 mg/日の併用療法に変更した．LVD耐性株にETVを使用した場合，高率にETV耐性株が出現すること，これまでに多剤使用歴を有することなどから，HBV DNAの逆転写酵素（RT）領域のアミノ酸配列を調べた．患者血清から抽出したHBV DNAをPCR法にて増幅した後，INNO-LiPA HBV DR（ver 2 plus ver 3）とdirect sequence法およびクローニング法にてウイルス変異を決定した（Table 2）．LVD耐性変異であるL80I，L180M，M204I/Vを有し，さらにADV耐性変異であるA181TとETV耐性変異であるL180M，T184I，M204I/Vも存在した．なお，クローニングの結果，RT領域domain BとCのmajorクローン配列はL180M＋A181T＋M204Iであり，minorクローンとしてL180M＋T184I＋M204Vが検出された．以上より，多剤耐性HBV株によるBTHと診断された．

```
Amino acid No. 71        80  84                                        120
   AB246345   NLLSSNLSWLSLDVSAAFYHIPLHPAAMPHLLVGSSGLPRYVARLSSTSR
 (1)2008/08   ----------I---M-----------------------------------
 (2)2009/02   ----------------------------------------------------

Amino acid No. 121                                                   170
   AB246345   NINYQHGTMQDLHDSCSRNLYVSLLLLYKTFGRKLHLYSHPIILGFRKIP
 (1)2008/08   ----------------------------------------------------
 (2)2009/02   ----------------------------------------------------

                    180 184
Amino acid No. 171      181        191          204              220
   AB246345   MGVGLSPFLLAQFTSAICSVVRRAFPHCLAFSYMDDVVLGAKSVQHLESL
 (1)2008/08   ----------MT--I------I-----------Ψ----------------
 (2)2009/02   ----------------------------------------------------

Amino acid No. 221             237                 256 260
   AB246345   FTSITNFLLSLGIHLNPNKTKRWGYSLNFMGYVIGCWGTL
 (1)2008/08   ----------------T-----------------S-----
 (2)2009/02   ----------------------------------S----
```

Ψ: I/V mixed type

**Fig. 2** Amino acid sequences alignment of HBV reverse transcriptase region at different times. The reference sequences indicate the amino acid sequences of HBV genotype C clone at GenBank accession number AB246345. The analyzed points are (1) at commencement of TDF/LVD (2008. 08) and (2) at 1 weeks after HSCT (2009. 02).

LVD＋ADV 併用療法開始7週時点の ALT は 196 IU/L と高値を維持し，また HBV DNA は 5.4 log copies/ml と 1 log 程度の減少に留まっていた．一方，B 型肝炎に対する治療継続中も呼吸困難感の改善を認めないことから，再発 DLBCL に対する可及的速やかな化学療法導入が必要不可欠であった．したがって，当院倫理委員会承認のもと，8月12日より ADV に変えて TDF 300 mg/日の投与を開始した．TDF＋LVD 併用療法の開始後より速やかな HBV DNA 量の低下と肝機能の改善を認め，DLBCL に対するサルベージ療法である化学療法（R-DeVIC 療法を3コース）と放射線療法（限局的照射野として上縦隔，左鎖骨窩，左頸部へ，total 24 Gy 照射）を速やかに施行することができた．年齢も若く，また実兄の HLA が一致していたため，引き続き同種骨髄移植（allogeneic hematopoietic stem cell transplantation：allo-HSCT）が検討された．しかし，同胞である兄も同様に HBV 無症候性キャリアであり，さらに血中 HBV DNA 量は 8.8 log copies/ml 以上と高値を示していた．移植ドナーとしては抗ウイルス剤使用によるウイルス量の低下を推奨したが[8]，ドナー本人から投与期間の明確でない核酸アナログ治療に対する同意が得られなかった．したがって，ドナー感染 HBV に薬剤耐性変異がないことを確認した後に，ウイルス量高値のまま 2009 年2月に allo-HSCT が行われた．HSCT 施行後に血中ウイルス量の上昇と肝酵素の上昇を認めたが，HBV DNA 塩基配列解析より当初レシピエントで認めた多剤耐性変異株は検出されず，ドナー由来の HBV 野生株による再感染が原因と考えられた（Fig. 2）．HBV 野生株であれば TDF＋LVD 併用療法が十分に効果を有すると考え，TDF＋LVD 併用療法が継続された．その後，血中ウイルス量はすみやかに低下し，以降 BTH の再燃なく現在まで経過し，さらに HSCT 後2年6カ月時点で DLBCL は完全寛解を維持している．

## 考　察

平成 23 年度のわが国のガイドラインでは，初回治療例への ETV 投与，および LVD 投与例でも HBV DNA 感度未満の場合は ETV への切り替えが推奨されている．しかし，ETV 切り替え例には微量の LVD 耐性ウイルスを有する症例も存在し，長期投与による ETV 耐性出

現の可能性は否定できない．また，LVD耐性例に対するADV併用療法の抗ウイルス効果は概ね良好であるが，一部の症例では治療効果が低く，投与期間の長期化により少数例ながら多剤耐性変異の出現が予測される．ガイドラインによれば，LVD，ADV，ETVのいずれの薬剤にも耐性株が出現した場合は，ETV＋ADV併用療法あるいはTDFを推奨している．しかしながら，わが国ではTDFはB型慢性肝炎に対する保険認可が無く，TDF使用症例の蓄積が乏しいため，現時点ではTDFの有効性に関する一般的な見解はない．

TDFはADVと類似した構造を有し，野生株ないしLVD変異株に対する*in vitro*での抗ウイルス効果は同程度とされている[9]．一方，TDFはADVに比較して腎障害の発生頻度が低く，ADVの30倍量の投与が可能であり[10]，優れた抗ウイルス効果を発揮することが期待されている．実際，ADV単独投与との二重盲検試験による治療成績では，TDF単独48週投与によるHBe抗原陽性例とHBe抗原陰性例におけるHBV DNA陰性化率は76%，93%であり，ADV単独療法の成績を有意に上回るものであった[10]．また，TDF耐性発現については3年間の継続投与で0%と報告されている[11]．

さらに海外から，LVDとADVの両薬剤耐性ウイルスに対するTDFを用いた治療がいくつか報告されている．Choeらは，LVD＋ADV併用療法中のvirologic breakthroughないし治療反応不良を示したB型肝硬変6例に対してTDF＋LVD併用療法を行ったところ，6例中5例ではrt181やrt236のADV耐性変異が確認されていたが，全例が12カ月以内にHBV DNAが感度以下となり，TDFが有効であったと報告している[12]．また，Bommelらの報告では，LVD，ADV使用131例に対して平均23カ月のTDF単独治療を行ったところ，1例もvirologic breakthroughを認めず，79%がHBV DNA感度以下に低下した．興味深いことに，LVD耐性変異に対するTDF治療効果は良好であったが，ADV耐性変異に対するTDF治療効果は減弱する(HBV DNA感度以下の割合は，LVD耐性変異例が100%に対して，ADV耐性変異例では52%)ことが報告されている[13]．一方，Pattersonらは，LVD治療不応かつADV治療反応不良の60例に対して，前治療がADV単独治療例はTDF単剤投与，ADV＋LVD併用例はTDF＋LVD併用投与とし，さらにTDF単独24週投与における反応不良例はTDF＋LVD併用に移行する前向き検討を実施している．結果は48週後に46%，96週後に64%がHBV DNA感度以下に低下し，またTDF使用前のLVD耐性変異rt204とADV耐性変異rt181やrt236による治療効果への影響はなかったと報告している[14]．

これらの報告は，多剤耐性症例に対してTDFが有効であることを示すとともに，ADV耐性変異出現例ではTDF単独投与による治療効果が減弱する可能性があることを示唆している．したがって，ADV耐性を既に有していた今回の症例では，TDF単独投与ではなくTDF＋LVD併用療法が選択された．

当症例は，ETVの登場に伴い，それまで経過良好であったLVD＋ADV併用療法からETV単独投与に治療変更された．ETV投与開始時点で耐性ウイルス検査は行われていないが，LVD治療中に発生したBTHのエピソードから，LVD耐性変異が既に存在することが予測される．LVD耐性変異獲得例におけるETVのgenetic barrierは低く，容易にETV耐性変異を獲得することが理解されるが，ETV発売当初はまだこのことが周知されておらず，服薬コンプライアンスおよびnaïve症例に対する強力な抗ウイルス効果のみを優先したETV単独療法への変更が一部で行われていた．現在の認識ではLVD耐性獲得症例にはADV add-on治療が原則であるが，当時の状況を考えると当症例のごとくETV単独への切り替え症例が少なからず存在することが予測され，今後は多剤耐性変異ウイルスの出現が危惧される．

また，合併する悪性リンパ腫に対して，HBVキャリアをドナーとしたHSCTが実施された．HBV陽性ドナーからの骨髄移植では，HBVが高率にレシピエントに感染するため，通常はドナーに対する核酸アナログによるウイルスコントロールとレシピエントに対するHBVワクチン投与が推奨されている[8]．しかしながら，当ケースでは移植前のウイルスコントロールに対するドナーの同意が得られず，さらにレシピエントは既にHBV感染が成立していることから，いずれの予防的処置も行うことはなかった．実際，移植後に一過性のウイルス量増加を認めたが，感染したウイルスはドナー由来の野生株であり，継続するTDF＋LVD併用療法により良好な経過を示した．我々が調べた限りでは，異なるHBV株の重複感染に対する核酸アナログ製剤の予防効果についての報告は少なく，その頻度は不明であるが，もし重複感染が成立した場合でも耐性変異がない薬剤を選択することによりHBVの増殖は抑制可能で，重篤な肝炎を併発する危険性は少ないことが予測される．